Fungal Genetics and Biology 140 (2020) 103368

Contents lists available at ScienceDirect

Fungal Genetics and Biology

journal homepage: www.elsevier.com/locate/yfgbi

Erg6 affects membrane composition and virulence of the human fungal pathogen *Cryptococcus neoformans*

Fabiana Freire M. Oliveira[a], Hugo Costa Paes[a], Luísa Defranco F. Peconick[b], Fernanda L. Fonseca[c], Clara Luna Freitas Marina[i], Anamélia Lorenzetti Bocca[i], Mauricio Homem-de-Mello[f], Márcio Lourenço Rodrigues[d,e], Patrícia Albuquerque[b], André Moraes Nicola[a], J. Andrew Alspaugh[g], Maria Sueli S. Felipe[h,1], Larissa Fernandes[b,i,1,*]

[a] Faculty of Medicine, Campus Darcy Ribeiro, University of Brasília, Asa Norte, Brasília, Federal District 70910-900, Brazil
[b] Faculty of Ceilândia, Campus UnB Ceilândia, University of Brasília, Ceilândia Sul, Centro Metropolitano, Brasília, Federal District 72220-275, Brazil
[c] Center for Technological Development in Health (CDTS), Fiocruz-RJ, Rio de Janeiro 21045-360, Brazil
[d] Carlos Chagas Institute, Fiocruz-PR, Curitiba 81310-020, Brazil
[e] Microbiology Institute, Federal University of Rio de Janeiro, Rio de Janeiro 21941-590, Brazil
[f] Faculty of Health Science, Campus Darcy Ribeiro, University of Brasília, Asa Norte, Brasília, Federal District 70910-900, Brazil
[g] Duke University School of Medicine, Dept. of Medicine, Durham, DUMC Box 102359, 303 Sands Building, Research Drive, Durham, NC 27710, USA
[h] Catolic University of Brasilia, Campus Asa Norte, SGAN 916 Módulo B Avenida W5, Asa Norte, Brasília, Federal District 70790-160, Brazil
[i] Laboratory of Applied Immunology, Institute of Biology, Room J1 28/8, Building J, 2nd Floor, Campus Darcy Ribeiro, University of Brasília, Asa Norte, Brasilia, Federal District 70910-900, Brazil

ARTICLE INFO

Keywords:
Sterol C-24 methyltransferase
Ergosterol
Virulence
Membrane sterol composition

ABSTRACT

Ergosterol is the most important membrane sterol in fungal cells and a component not found in the membranes of human cells. We identified the *ERG6* gene in the AIDS-associated fungal pathogen, *Cryptococcus neoformans*, encoding the sterol C-24 methyltransferase of fungal ergosterol biosynthesis. In this work, we have explored its relationship with high-temperature growth and virulence of *C. neoformans* by the construction of a loss-of-function mutant. In contrast to other genes involved in ergosterol biosynthesis, *C. neoformans ERG6* is not essential for growth under permissive conditions in vitro. However, the *erg6* mutant displayed impaired thermotolerance and increased susceptibility to osmotic and oxidative stress, as well as to different antifungal drugs. Total lipid analysis demonstrated a decrease in the *erg6*Δ strain membrane ergosterol content. In addition, this mutant strain was avirulent in an invertebrate model of *C. neoformans* infection. *C. neoformans* Erg6 was cytolocalized in the endoplasmic reticulum and Golgi complex. Our results demonstrate that Erg6 is crucial for growth at high temperature and virulence, likely due to its effects on *C. neoformans* membrane integrity and dynamics. These pathogen-focused investigations into ergosterol biosynthetic pathway components reinforce the multiple roles of ergosterol in the response of diverse fungal species to alterations in the environment, especially that of the infected host. These studies open perspectives to understand the participation of ergosterol in mechanism of resistance to azole and polyene drugs. Observed synergistic growth defects with co-inhibition of Erg6 and other components of the ergosterol biosynthesis pathway suggests novel approaches to treatment in human fungal infections.

1. Introduction

Ergosterol is a major sterol component found mainly in fungal membrane (Kristan and Rižner, 2012). Recent investigations have focused not only on the function of ergosterol as a structurally rigid component of the plasma membrane, but also as a key regulator of complex aspects of cell physiology (Koselny et al., 2018; Rodrigues, 2018). Besides acting as an important component of cellular

* Corresponding author at: Laboratory of Applied Immunology, Institute of Biology, Room J1 28/8, Building J, 2nd Floor, Campus Darcy Ribeiro, University of Brasília, Asa Norte, Brasilia, Federal District 70910-900, Brazil.
E-mail addresses: fernandalof@micro.ufrj.br (F.L. Fonseca), albocca@unb.br (A.L. Bocca), mauriciohmello@unb.br (M. Homem-de-Mello), andrew.alspaugh@duke.edu (J.A. Alspaugh), larissaf@unb.br (L. Fernandes).
[1] L.F and M.S.S.F. share senior authorship of this article.

https://doi.org/10.1016/j.fgb.2020.103368
Received 24 September 2019; Received in revised form 12 February 2020; Accepted 17 February 2020
Available online 19 March 2020

membranes, the sterols regulate diverse biologic processes by affecting signal transduction, cytoskeleton organization, cell growth, vesicle transport and virulence (Dufourc, 2008; Hannich et al., 2011; Kristan and Rižner, 2012; Parks and Casey, 1995). Recently, ergosterol was defined as an immunologically active molecule that influences innate immune activation and macrophage pyroptosis (Koselny et al., 2018).

The absence of ergosterol enhances the membrane fluidity, which is responsible for increasing diffusion of various drugs. Polyenes and azoles are two antifungal classes that impair ergosterol function in the fungal cell membrane. The first drug group, exemplified by amphotericin B, directly targets ergosterol in the membrane, and causes cell injury by multiple means, including physically depleting membrane ergosterol, forming pores causing leakage of intracellular cations, and inducing the accumulation of reactive oxygen species (ROS) within the cell (Mesa-Arango et al., 2014). In contrast, azoles directly inhibit Erg11/CYP51, an intermediate enzyme of sterol biosynthesis. The ergosterol biosynthetic pathway enzymes have attracted many studies to identify new drug targets; however, a serious concern is that some of them are also shared with cholesterol biosynthesis pathways in mammalian cells (Daum et al., 1998; Espenshade and Hughes, 2007; Kristan and Rižner, 2012).

Ergosterol biosynthesis and its regulation have been studied in most detail in the yeast model *Saccharomyces cerevisiae* (Dupont et al., 2011; Gaber et al., 1989; Hu et al., 2017; Jacquier and Schneiter, 2012; Parks and Casey, 1995; Servouse and Karst, 1986). In contrast, less is known about this process in fungal pathogens such as *C. neoformans* (Chang et al., 2009; Kim et al., 1975; Nes et al., 2009; Toh-e et al., 2017). The terminal steps of sterol production in *S. cerevisiae* occur in the endoplasmic reticulum (ER). Afterwards, ergosterol molecules are transferred as steryl-esters to different subcellular compartments such as the plasma membrane and endomembrane system of peroxisomes, mitochondria, vacuoles and the ER where they are found as free sterols (Alvarez et al., 2007; Jacquier and Schneiter, 2012; Parks and Casey, 1995). The metabolic conversion between sterols and fatty acids and their transport through the cell is still not completely defined for many fungi. Sterols are closely associated with unsaturated fatty acids and distributed asymmetrically in plasma membrane microdomains known as lipid “rafts” and packed in a liquid-ordered state, which is responsible for maintaining the membrane micro fluid state (Dufourc, 2008; Wachtler and Balasubramanian, 2006). Previous studies revealed the presence of sterol-rich domains in the bud tips of *C. neoformans* (Nichols et al., 2004), suggesting that lipid “rafts” may regulate fungal morphology, and also may play a role in pathogenicity by exposing virulence factors on membrane (Farnoud et al., 2015).

Cryptococcosis is a disease that affects primarily immunocompromised hosts, mainly occurring in the setting of HIV/AIDS, chemotherapy and transplant patients. Globally, it is estimated that 181,000 patients die of cryptococcal meningitis each year, with most cases occurring in resource-limited regions of the world with concomitant high incidences of HIV infection (Rajasingham et al., 2017). *Cryptococcus neoformans* is one of the related species that causes cryptococcosis, a disease initiated by the inhalation of an infectious propagule, and most often resulting in an asymptomatic pulmonary infection. However, in the setting of immunosuppression, this opportunistic fungal pathogen can disseminate to the central nervous system leading to lethal meningoencephalitis (reviewed in (Maziarz and Perfect, 2016)).

The Erg6 enzyme catalyzes steps of the ergosterol synthesis pathway that are unique for sterol biosynthesis in fungi, plants and some protozoa (Weete et al., 2010). *C. neoformans ERG6* encodes a 24-C-methyltransferase that converts zymosterol into fecosterol, the first step in the ergosterol pathway that diverges from cholesterol biosynthesis (Nes et al., 2009). Erg6 also acts in the alternative pathway of ergosterol biosynthesis to convert lanosterol to eburicol (Nes et al., 2009). Mutants with loss-of-function in *ERG6* have been studied in other fungi, mainly ascomycetes, such as *S. cerevisiae* (Gaber et al., 1989), *Candida albicans* (Jensen-Pergakes et al., 1998), *Candida lusitaniae* (Young et al., 2003), *Candida glabrata* (Vandeputte et al., 2007) and *Kluyveromyces lactis* (Konecna et al., 2016). Although *ERG6* is not an essential gene for those microorganisms, its absence resulted in a variety of compromised phenotypes related to membrane permeability and fluidity, alterations in the susceptibility to different antifungal compounds, impairment in cell wall integrity, and accumulation of sterol intermediate compounds (Gaber et al., 1989; Jensen-Pergakes et al., 1998; Konecna et al., 2016; Vandeputte et al., 2007; Young et al., 2003).

Although the role of Erg6 on membrane properties and its impact on fungal physiology has been widely characterized in ascomycetes, its role in basidiomycetes and diverse fungal pathogens is less well explored. Recently, Toh-e et al. constructed a selection of *C. neoformans erg* mutants to assess the effect of ergosterol defects on the cellular response to treatment with antifungal drugs targeting cell wall processes (Toh-e et al., 2017). This study builds upon prior work to more fully examine the involvement of *C. neoformans* Erg6 in ergosterol homeostasis, membrane composition and pathogenesis. Finally, based on the fact the membranes of fungi and humans are fundamentally different in the sterol content, and that ergosterol is such an important structural and active molecule related to several fungal biological process, we propose that fungal-specific components of sterol synthesis, such as Erg6, may offer unique insight into mechanisms of adaptive environmental responses and potential targets for antimicrobial development.

2. Materials and methods

2.1. 1. Media, cell line and strains

The H99 strain of *C. neoformans* var. *grubii* serotype A was used as the wild type strain and also to generate the *erg*6Δ mutant and the reconstituted strains *erg*6Δ + *ERG6* (corresponding to CNAG_03819) (Table S1). The strains were kept at −80 °C and freshly streaked for single colonies every week on YPD agar plates (1% yeast extract, 2% bacto peptone, and 2% dextrose [pH 5.6]). The cells were incubated at 30 °C for 48 h unless noted otherwise. The murine macrophage line J774A.1 was maintained at 37 °C in 5% CO2 in Dulbecco’s modified Eagle’s medium (DMEM) (Gibco BRL), supplemented with 10% heat-inactivated fetal calf serum (Gibco BRL). DH5α *Escherichia coli* competent cells were used for plasmid manipulations.

2.2. In silico search for enzymes related to ergosterol biosynthesis in C. neoformans

The ergosterol biosynthesis pathway presents some differences among fungal species (Weete et al., 2010). The *C. neoformans* ergosterol pathway was proposed by Nes and colleagues (Nes et al., 2009), and we compared that to others proposed in the literature and also the ones indicated in the database FUNGIpath v3.0 of KEGG. Finally, we used BLASTp to search for enzyme sequences of the pathway using the Broad Institute *C. neoformans* var. *grubii* H99 Database (http://www.broadinstitute.org/annotation/genome/cryptococcus_neoformans/MultiHome.html).

2.3. Mutant construction by Double-Joint PCR (DJ-PCR), locus reconstitution and yeast transformation

ERG6 sequence (CNAG_03819, GenBank ID: 23887278) was obtained from Broad Institute *C. neoformans* var. *grubii* H99 Database. Homology searches suggest that this gene encodes a highly conserved sterol 24-C-methyltransferase which is located in chromosome 2, supercontig 2 from 922605 to 924403 + strand. The deletion cassette was generated by DJ-PCR as previously described (Kim et al., 2009) using the Hygromycin B resistance marker, *HPH* (Hygromycin Phosphotransferase gene) under control of the actin *ACT1* promoter and *TRP1*

terminator (Walton et al., 2005). Firstly, four fragments were amplified, two of them corresponding to the 5′- and 3′- flanking regions of the *ERG6* gene, using the primers LF042/LF043 (5′*ERG6* – 840 bp) and LF044/LF045 (3′*ERG6* 849 bp), and the template was H99 genomic DNA. The 5′ and 3′ regions corresponding to the *HPH* marker were also amplified with the primers LF046/LF028 (5′*HPH* – 1235 bp) and LF029/LF057 (3′*HPH* – 1,263 bp) from the pZPHYG2 (Walton et al., 2005) as template. The second round of PCR was carried out to join the fragments 5′*ERG6* and 5′*HPH* (LF042/LF028 – 2,075 bp) and 3′*ERG6* and 3′*HPH* (LF029/LF045 – 2,112 bp) (a detailed schema is found in Fig. S1A–B). The primer sequences are listed in Table S2. All amplifications were performed using *Fast DNA Polymerase* (Fermentas) as follows: 1 × Fast Polymerase (Fermentas); 0.5 μM of each primer; 10 ng of genomic DNA from H99 strain or 10 ng of pZPHYG2. 10 ng of each fragment from the first round PCR were used subsequently for the overlap PCR. The two DJ-PCR fragments were purified by GFX purification kit (GE Healthcare) and co- transformed by biolistics into H99 yeast cells from *C. neoformans*. Several colonies were obtained and the ones resistant to Hygromycin B at 200 μg/mL (Invitrogen) were selected. To reintroduce the wild-type *ERG6* locus into the *erg*6Δ mutant strain, the cassette containing the *ERG6* gene was amplified using primers LF042/LF045, 3,447 bp. This fragment was co-transformed with pJAF1 (G418 - neomycin phosphotransferase resistance mark, controlled by *C. neoformans* actin promoter and terminator) into the *erg*6Δ strain by biolistic transformation. Several colonies with different features were obtained and those G418-resistant (200 μg/mL) and Hygromycin B-susceptible were selected.

The biolistic transformations were performed as previously described (Toffaletti et al., 1993). Briefly, culture of *C. neoformans* grown overnight in 50 mL of YPD liquid medium was washed with 0.9% NaCl and spread on YPD + 1 M Sorbitol (Vetec) plates. DNA samples were prepared with 50 μL sterile Tungsten microcarrier beads 60 mg/mL (0.7 μm, Bio-Rad) with 1 μg of DNA, 50 μL of 2.5 M $CaCl_2$ (Sigma) sterile, and 20 μL of 0.1 M Spermidine (Sigma). The mixture was vortexed for 10 min, then centrifuged, washed twice with 150 μL of absolute ethanol. The beads carrying the DNA were suspended in absolute ethanol and distributed on macrocarrier disks. Bombardment of the plates by biolistic transformation apparatus (Biorad) followed the manufacturer's instructions with helium gas pressure of approximately 1,200 psi under 27 mmHg. The plates were incubated for 24 h at 30 °C; then the cells were washed and transferred to appropriate selective medium and incubated at 30 °C until the colonies appeared on the agar surface. The mutant or reconstituted colonies were screened by PCR. Genomic DNA from selected transformants was used as a PCR template to confirm the correct insertion of the deletion cassette or *ERG6* gene. PCR confirmation of correct integration of HPH cassette into the locus of *ERG6* used the combination of the primers LF36/LF28 (2355 bp) and LF029/LF037 (2963 bp) as detailed in Fig. S1C–D. Confirmation of *ERG6* locus reconstitution was carried out with primers LF036/LF041 (2701 bp) and LF037/LF040 (1973 bp) Fig. S1E. The strains constructed in this study and the respective selective marker are in Fig. S2.

2.4. Southern blotting

Based on the predicted *ERG6* genomic sequence (cneoH99_Chr2 910000–935000), the restriction enzyme profile was analyzed and BglII and XhoI were selected. 10 μg of genomic DNA was extracted, restriction enzyme digested overnight at 37 °C, and electrophoresed in a 0.8% TAE 1X agarose gel. The gel was blotted onto a charged nylon membrane (GE Healthcare) by upward capillary transfer. Amplification of probe used the primers LF40/LF45 (1099 bp) and was labelled with the PCR DIG Probe Synthesis Kit (Roche). Hybridization and membrane washes were carried out using DIG Easy Hyb Granules and DIG wash and Block solution Set, respectively (both from Roche). For detection Anti-Digoxigenin-AP, Fab fragments from sheep and CDP-Star ready-to-use were used (both from Roche). All procedures were based on the suppliers' recommendations.

2.5. Real time PCR

Total RNA was extracted from H99, *erg*6Δ and *erg*6Δ + *ERG6* strains using TRI- Reagent (Applied Biosystem). cDNAs were synthesized with High Capacity cDNA Reverse Transcription kit (Applied Biosystems) for a 20 μL final volume reaction. To quantify *ERG6* expression by Real-time PCR (equipment 7500 Fast Real Time PCR System - Applied Biosystems) the Fast SYBR® Green Master Mix kit (Applied Biosystems) was employed, based on the suppliers' protocols. The primers LF40/LF41 and LF38/LF39 were designed in the exon-exon junction for *ERG6* and ACTIN (*ACT1*) amplification, respectively. *ACT1* was used as a housekeeping gene for sample normalization. Relative quantification was calculated using the CT comparative method ($2^{-\Delta\Delta\ CT}$).

2.6. Phenotypic assays

The strains H99, *erg*6Δ and *erg*6Δ + *ERG6* were grown overnight at 30 °C in YPD liquid medium, washed with 0.9% NaCl and serially diluted from 10^7 to 10^3 cell/mL. 5 μL of each dilution were spotted on YPD agar supplemented with the respective stressor agent. Susceptibility to high temperature was evaluated by incubating the plates at 30 or 37 °C for 48–72 h. Cell wall integrity was analyzed using Congo Red 1 and 0.5%, Caffeine 1 mg/mL and 0.5 mg/mL, Calcofluor White 1 mg/mL or 0.5 mg/mL and 0.05% of SDS (all from Sigma). Osmotic stress was induced by 1.5 M of NaCl and 1.5 M KCl. Sensitivity to Hydrogen peroxide was tested in YPD plates with 1 mM and 5 mM of H_2O_2. The plates were incubated at 30 °C for four days and then photographed. Phospholipase production was visualized on Agar plates with Egg emulsion (Price et al., 1982) and 10^7 yeast dilution was spotted, and incubated at 35 °C for 48 h. The enzymatic activity of phospholipase (Pz) was measured by the ratio of colony diameter (DC) to colony diameter plus precipitation zone (DCP). Accordingly to Djordjevic (Djordjevic, 2010) if the result is $Pz = 1$, the activity is considered negative; $1 > Pz > 0.64$ the activity is positive and $Pz < 0.64$ means it is strongly positive. Ability to produce melanin was observed in L-DOPA agar plates. To detect any morphological cellular alterations related to the high temperature incubation, the strains were subjected to overnight growth on liquid YPD at 30 °C, 150 rpm, following a saline wash of the pelleted cells, resuspension in a new liquid YPD and re-incubation at 37 °C, 150 rpm for 4 and 16 h. After these periods, the cells were microscopically visualized in an inverted epi-fluorescence microscope Zeiss Axio Observer Z1 equipped with a 63 × NA 1.4 oil immersion objective and cooled CCD camera.

2.7. Analysis of capsule and its main component GXM

The capsule production was evaluated on liquid Minimal Medium (10 mM $MgSO_4$, 29.3 mM KH_2PO_4, 13 mM glycine, 3 μM thiamine-HCl, 15 mM glucose, pH 5.5). Polysaccharide isolation was performed as described by Nimrichter and colleagues (Nimrichter et al., 2007). Briefly, fungal cells were cultivated under agitation for 2 days at room temperature and separated from culture supernatants by centrifugation. The culture supernatants fluids were centrifuged at 15,000*g* (15 min, 4 °C) for clarification and concentrated approximately 20-fold using an Amicon (Millipore, Danvers, MA) ultrafiltration cell (cutoff = 100 kDa). The fluid phase was discarded, and the viscous layer was collected with a cell scraper for further analysis of zeta potential, molecular dimensions and serological quantification. Effective diameter and size distribution of GXM (glucuronoxylomannan) preparations from H99, *erg*6Δ and *erg*6Δ + *ERG6* cells were measured by quasi-elastic light scattering in a 90Plus/BI-MAS Multi Angle Particle Sizing analyzer (Brookhaven Instruments Corp., Holtsville, NY (Frases et al., 2009). Multimodal size distribution analysis of polysaccharides was calculated from the values of intensity weighted sizes obtained

from the non-negatively constrained least squared (NNLS) algorithm. Zeta potential was calculated in a Zeta potential analyzer (ZetaPlus, Brookhaven Instruments Corp., Holtsville, NY) as described previously (Fonseca et al., 2009a). For visual analysis of cellular GXM and associated structures, the strains were stained for GXM, chitin and chitooligomers (Fonseca et al., 2009b). The cells were first suspended in 100 µL of a 5 µg/mL solution of the Alexa Fluor 594 conjugate of the wheat germ agglutinin (WGA, chitooligomer staining) and incubated for 30 min at 37 °C. After the cells were washed in PBS, they were incubated with 25 µM calcofluor white (chitin staining) under the same conditions. The cells were then washed in PBS and suspended in a 10 µg/mL solution of mAb 18B7 in PBS, kindly provided by Dr. Arturo Casadevall (Johns Hopkins University). MAb18B7 is an IgG1 that recognizes all GXM serotypes (McFadden and Casadevall, 2004). After 1 h of incubation and subsequent washing, yeast cells were incubated with a fluorescein isothiocyanate (FITC)-labeled goat anti-mouse IgG (Fc specific) antibody, washed with PBS and placed in mounting medium (50% glycerol and 50 mM *N*-propyl gallate in PBS) over glass slides. Images were acquired in an Axioplan 2 (Zeiss, Germany) fluorescence microscope using a Color View SX digital camera and processed with the software system analySIS (Soft Image System). Extracellular quantification of GXM was performed by ELISA according to Casadevall et al. (Casadevall et al., 1992) with minor modifications (Nimrichter et al., 2007).

2.8. Growth curve assays

The growth of the H99, *erg*6Δ and *erg*6Δ + *ERG6* strains was quantified at 30, 35 and 37 °C in YPD liquid medium. Additionally, the strains were also grown in YNB liquid medium at 30 °C. The cells were grown on YPD liquid medium overnight at 30 °C, under agitation, washed with 0.9% NaCl, and the final concentration adjusted to 1×10^6 yeast cells in 96-well plates in YPD or YNB. To evaluate ability to grow at high temperature, the strains *erg*6Δ + *ERG6*-GFP, *erg*6Δ + GFP and the controls (H99, *erg*6Δ and *erg*6Δ + *ERG6*) were inoculated in 96-well plates in YPD at 1×10^4 yeasts per well. The plates were incubated under continuous agitation and optical density was measured every 30 min at 600 nm by *Eon biotek* spectrophotometer for about 96 h.

2.9. Antifungal susceptibility tests

The susceptibility of H99, *erg*6Δ and *erg*6Δ + *ERG6* strains to different drugs was observed on YPD agar plates supplemented with each drug. 5 µL of serial dilutions from 10^7 to 10^3 cell/mL were spotted. The drugs were fluconazole 10 µg/mL, AmB 0.5, 1.0, 2.0, 4.0 and 8 µg/mL, itraconazole 0.012 µg/mL, ketoconazole 1 µg/mL, FK506 1 µg/mL, nystatin 50 µg/mL, cerulenin 10 µg/mL, brefeldin A 10 µg/mL, terbinafine 1 µg/mL (all of them purchased from Sigma). Furthermore, Minimal Inhibitory Concentration was determined by micro dilution in 96 well plates according to CLSI M27-A3 protocol (CLSI, n.d.). The growth of the strains was analyzed after 48 h by spectrophotometry at 595 nm.

2.10. Phagocytosis assay

Macrophage J744.A1 cells were used to evaluate survival of yeasts within mammalian cells as previously described (Cox et al., 2003). Anti-GXM mAb18B7- opsonized *C. neoformans* yeast cells were co-incubated in 96-well tissue culture plates with J774A.1 cells in 200 µL DMEM medium supplemented with 10% fetal bovine serum (the effector-to-target ratio was about 10:1, 10^6 yeast cells of *C. neoformans*, and 10^5 J774A.1 cells/200 µL). Phagocytosis rate was measured as the percentage of macrophages containing yeast cells, counted in three randomly chosen microscopic fields. The J774A.1 cells were activated by adding 100 U/mL interferon-gamma and 300 ng/mL of LPS one day prior to introducing the fungal cells. The plate was incubated at 37 °C for 2 h and the non-internalized fungal cells were removed by washing 3 × with PBS, and fresh medium was added, with the plate incubated overnight at 37 °C in 5% CO_2 atmosphere. The next day, macrophages were lysed by washing three times in sterile water. The yeast suspension was collected and plated on YPD agar to determine the number of *C. neoformans* viable cells. The agar plates were incubated at 30 °C and CFUs (Colony Forming Units) were counted after about 48 h. Data were analyzed using 2 -way ANOVA in GraphPad Prism 5. P value < 0.05 was considered significant. The experiments were performed in triplicate.

2.11. In vivo virulence assays

The virulence tests were performed with the *in vivo* wax moth model *Galleria mellonella* (Peleg et al., 2009). Yeast cells were kept overnight at 30 °C in YPD liquid medium and were re-suspended at 5×10^6 cells/mL in PBS. Groups of 16 final stage larvae were weighed and inoculated with 10 µL of H99, *erg*6Δ and *erg*6Δ + *ERG6* yeast suspensions using a Hamilton syringe into the last hind paw. PBS was injected as control. After injection, caterpillars were incubated in Petri dishes at 30 and 37 °C, and the number of dead caterpillars was scored daily based on the spontaneous or provoked motion. Survival curves were analyzed using log-rank and Wilcoxon tests using Graphpad 8.0.

2.12. Sterol analysis

The total lipids extraction was performed according to a protocol described previously (Folch et al., 1957). Briefly, yeast cells grown in YPD liquid medium at 30 °C for 48 h were washed three times with PBS, frozen at −80 °C and lyophilized for 10 h. For each sample were added glass beads (425–600 µm – Sigma) and a mixture of chloroform/methanol (2:1). The mixture was stirred, and the solvent was washed with 0.2 volumes of 0.9% NaCl solution. The sample was centrifuged at 500*g* and the lower phase was collected. The solvent evaporation was performed in a speed vacuum and the lipids were stored at −80 °C under protection of light. The lipids quantification was performed on a Shimadzu Liquid Chromatograph ® with an autosampler SIL-20SA with a loop of 100 µL, degasser system DGU-20A, quaternary pump system LC-20AT, oven CTO-20SAC, detector SPD-M20A, communicator module CBM-20A and LC solution software ® (Kyoto, Japan). The elution was performed in an isocratic way with HPLC grade methanol (Tedia) at a flow rate of 1.0 mL/min. The column was a C18 RP-ACE, 125 mm × 4.6 mm with 5 µm particles of average size. Two standard solutions for comparison of peak retention times were used in this analysis, lanosterol (10 µg/mL) and ergosterol (50 µg/mL), both from Sigma. The volume injected was 10 µL for most analyses, except for the tests with standard lanosterol, which were injected with 20 µL. The detector was SPD-M20A, PDA type (photo diode array) operating in 220 nm and 281 nm, optimal wavelengths to lanosterol and ergosterol, respectively. Peak areas were used to quantify both sterols. Calibration curves were obtained from standard solutions, ranging 0.1 µg/mL to 100 µg/mL. Linear correlation coefficients (r^2) above 0.99 were found to both curves.

2.13. Extracellular vesicles isolation

For extracellular vesicles (EV) isolation, one colony of each strain was inoculated at Sabouraud Dextrose Broth (SDB) for 48 h at 30 °C under agitation at 120 rpm. Then, the cells were counted and diluted to a density of 3.5×10^7 cells/mL and 300 µL was spread at Sabouraud Dextrose Agar (SDA) plates, and subjected to incubation at 30 °C for 24 h. Then, the yeast cells were collected using a cell scraper and deposited in phosphate-buffered saline (PBS). Cell suspensions were sequentially centrifuged to remove yeast cells and possible debris, and the remaining supernatants were filtered at 0.45 µm syringe filter. To

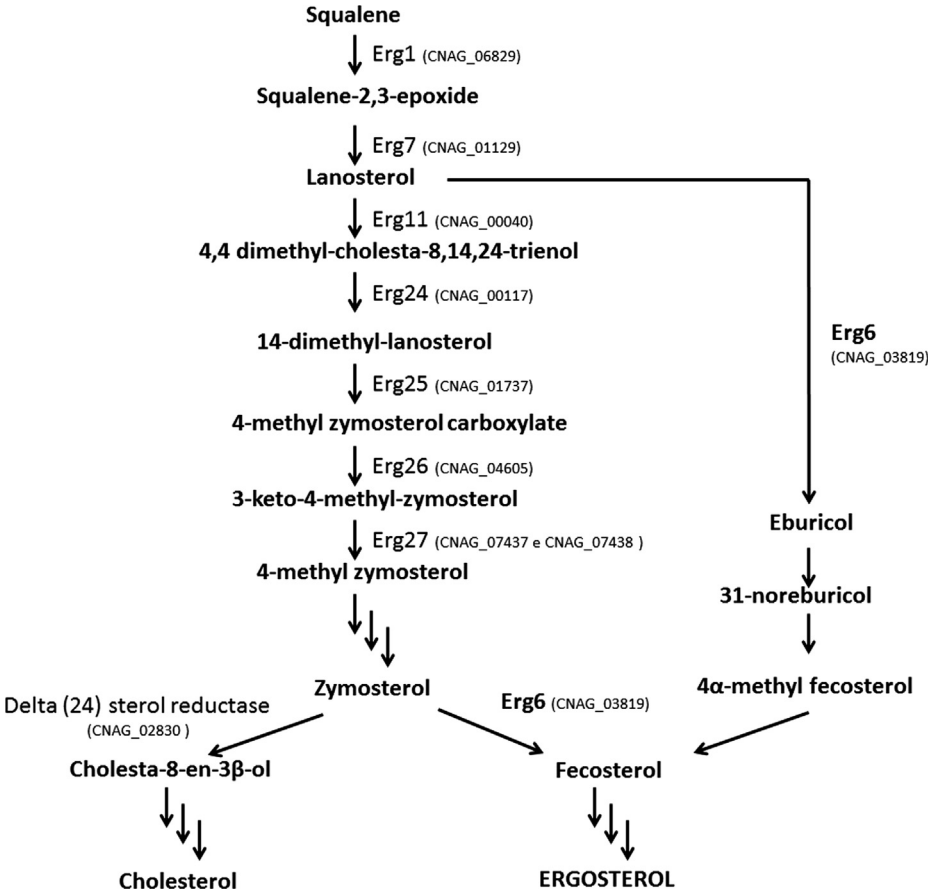

Fig. 1. Putative ergosterol biosynthesis pathways in *C. neoformans*. The most common pathway in fungi to produce ergosterol is via zymosterol. An alternative pathway uses eburicol. Erg6, a sterol-24-C-methyltransferase, is a common enzyme of both pathways to generate ergosterol. Erg1: squalene monooxygenase; Erg7: lanosterol synthase, Erg11: sterol 14-demethylase; Erg24: delta (14) sterol reductase, Erg25 is methylsterol monooxygenase, Erg26: sterol-4-alpha-carboxylate 3-dehydrogenase, Erg27: 3-keto-sterol reductase. The CNAG refers to the genomic sequence of Broad Institute Database H99 Genome Project.

collect EVs, the filtrate was ultra centrifuged at 100.000*g* for 1 h and the pellet was resuspended at 300 μL (Reis et al., 2019). The vesicles suspension also contained GXM, and to eliminate the maximum of capsular GXM, a capture ELISA was made, using the mAb 18B7. Total sterol and protein content were measured using colorimetric assays Amplex Red Cholesterol assay kit and Micro BCA Protein assay kit, respectively (both by Thermofisher Scientific) following manufacturer's instructions. To analyze vesicles hydrodynamic diameters we used Dynamic Light Scattering (DLS) "Zetasizer Nano ZS". Two independent experiments were performed in triplicate.

2.14. Erg6 cyto-localization experiments

To localize the Erg6 protein, the 1,032 bp fragment corresponding to the *ERG6* cDNA was amplified using the primers containing BamHI restriction sites (LF100/LF101) and was sub-cloned into the pGEM-T plasmid (Promega). The vector was digested with BamHI (Biolabs) and the insert cloned into the BamHI site of the pCN50 plasmid to produce a fusion of Erg6 with GFP (green fluorescent protein). This vector contains the resistance marker G418 - neomycin phosphotransferase resistance mark, controlled by actin promoter and terminator of *C. neoformans* and fluorescent marker *GFP* controlled by histone H3 promoter (O'Meara et al., 2010). Finally, 5 μg of pCN50 containing *ERG6* fused to GFP was transformed by biolistic in the *erg*6Δ mutant of *C. neoformans* and an empty pCN50 was used as control. The YPD agar plates were incubated for 24 h at 30 °C. The cells were washed and transferred to YPD agar containing 200 μg/mL of Hygromycin B or 200 μg/mL of G418. The colonies that were able to grow on plates containing both drugs were selected for analysis of fluorescence. The selected colonies were checked for wild type phenotype: ability to grow at 37 °C and on different concentrations of Amphotericin B to evidence the *ERG6* expression was restored (Fig. S5; Fig. 8). The cells were submitted to overnight growth in YPD liquid medium at 30 °C, under agitation, and the cells were collected and observed in an inverted epifluorescence microscope Zeiss Axio Observer Z1 equipped with a 63 × NA 1.4 oil immersion objective and cooled CCD camera. Five different dyes were used to determine the location the Erg6 fused to GFP by co-localization: Mitotracker orange (Invitrogen), BODIPY-Ceramide (Invitrogen), ER-Tracker (Invitrogen), FM-4-64 (Invitrogen) and Calcofluor White. Cells were incubated overnight at 30 °C in YPD, washed and diluted for a concentration 10^6 cells/mL. The treatment of yeast cells consisted of: 100 nM Mitotracker for 1 h at 30 °C; 5 μM Bodipy-Ceramide for 10 min at 4 °C, 10 μM ER-Tracker for 20 min at 30 °C, 10 μg/mL of FM-4-64 for 30 min at 37 °C and 5 μg/mL of Calcofluor White for 1 h at 30 °C. Before microscopic visualization, the cells were washed three times in PBS. Images were collected with the Zeiss ZEN software. The resulting images were processed with ImageJ and Adobe Photoshop software. Brightness and contrast were adjusted on the DIC images; no non-linear manipulations were made in the images.

3. Results

3.1. In silico analysis of ergosterol biosynthetic pathway in C. neoformans

Ergosterol synthesis is a result of a cascade with over 20 enzymatic reactions, which starts with the reaction of two acetyl-CoA molecules catalyzed by the enzyme acetoacetyl-CoA thiolase, encoded by *ERG10*. The difference between the cholesterol and ergosterol pathways starts with the conversion of zymosterol to fecosterol by Erg6 (Daum et al., 1998). After fecosterol formation, it is converted into episterol, which generates ergosta-5,7,24(28)-trienol, ergosta-5,7,24(28)-trienol, which is converted to ergosta-5,7,22,24(28)-tetraenol and finally to ergosterol, by the enzymes sterol-C-24-methyltransferase (Erg6), sterol-C-8-isomerase (Erg2), sterol-C-5-desaturase (Erg3), sterol-C-22-desaturase

(Erg5), and sterol-C-24-reductase (Erg4), respectively (Daum et al., 1998). Although ergosterol is a fungal sterol, the sterol pathway can vary and generate different intermediate products among fungal species (Weete et al., 2010). A general pathway to synthesize ergosterol starting with the conversion of squalene to lanosterol has been described by many authors to occur in fungi as diverse as *S. cerevisiae* (Gachotte et al., 1998; Hu et al., 2017; Parks and Casey, 1995; Servouse and Karst, 1986), *Candida albicans* (Sanglard et al., 2003), *Aspergillus fumigatus* (Alcazar-Fuoli et al., 2008), *Sporothrix schenckii*, *Sporothrix brasiliensis* (Borba-Santos et al., 2016) and *Schizosaccharomyces pombe* (Iwaki et al., 2008), and others. For *C. neoformans*, Erg6 also participates in an alternative pathway that produces eburicol and, at the end, ergosterol (Nes et al., 2009, 2008). Based on these previous studies, our analysis of the *C. neoformans* genome database identified genes encoding possible pathway components to generate ergosterol in *C. neoformans*. The respective enzymes are depicted in Fig. 1. By KEGG analysis, we observed well-conserved pathway components among the Basidiomycetes, in accordance with previously described observations (Toh-e et al., 2017).

3.2. Disruption and reconstitution of ERG6

An *ERG6* mutant strain (*erg*6Δ) was generated by homologous recombination in the H99 strain background. To confirm precise replacement of the *ERG6* locus by the mutant allele, we used both PCR and Southern blotting (Fig. S1A–D, Fig. 2). The Southern blot revealed no ectopic integrations (Fig. 2) and the expected hybridization pattern after DNA digestion with BglII and XhoI was visualized. To ensure that all phenotypes observed in the *erg*6Δ strain were due to gene deletion, we reintroduced the *ERG6* gene into the original locus of *erg*6Δ mutant to create the reconstituted strain *erg*6Δ + *ERG6*. The reconstitution of the locus was confirmed by PCR (Fig. S1E). In additional, a quantitative real-time PCR showed the mutant did not express *ERG6* while the reconstituted strain demonstrated restored *ERG6* expression (Fig. S1F). As demonstrated in Fig. S2 the mutant and reconstituted strains did express the expected antibiotic susceptibility pattern according to the selective marker used.

3.3. C. neoformans main virulence traits were not significantly affected by ERG6 deletion

The capsule is the main well-characterized virulence factor of *C. neoformans*, acting to physically protect the cells by avoiding dehydration and playing many important roles during the interaction with mammalian and invertebrate hosts (Zaragoza et al., 2009). The *erg*6Δ strain capsule size was similar when compared to the wild type, after induction in minimal medium, and by direct microscopic visualization with India ink counterstaining (Fig. 3A). Capsular polysaccharide features were further analyzed by assessing one of its main components, GXM. Microscopic examination of wild type, mutant and reconstituted strains revealed similar capsular architecture and dimensions, as demonstrated by similar pattern of immunofluorescence after staining with fluorescently labelled 18B7 antibody (directed against GXM) (Fig. 3A). The amount of extracellular GXM produced by all strains was also similar (Fig. 3C). *ERG6* deletion tended to slightly increase the negative charge of GXM, although no statistically significant alterations between zeta potential values obtained from wild type and mutant cells were observed (Fig. 3D). Finally, *ERG6* deletion did not affect GXM dimensions, as concluded from the similar profile of size distribution of polysaccharide fractions obtained from *erg*6Δ, wild type and *erg*6Δ + *ERG6* cells evaluated by DLS (Fig. 3E). Other virulence factors of *C. neoformans* were also assessed. No difference was noted for melanin production on L-DOPA agar plates (Fig. 3B upper panel). The *erg6* mutant secreted phospholipases on egg yolk agar medium. However the phospholipid degradation halo around the colonies was slightly but reproducibly smaller in *erg*6Δ than wild type and *erg*6Δ + *ERG6* strains (Fig. 3B bottom panel) (Pz values for wild type, reconstituted and mutant strains are 0.52, 0.47 and 0.73, respectively). Altered phospholipase secretion is often attributed to impairment of protein transport or problems in maintaining the integrity of the membrane and cell wall (Siafakas et al., 2007).

3.4. Erg6 is required for high temperature growth

To assess the role of Erg6 in thermotolerance, serial dilutions of *erg*6Δ, wild type and *erg*6Δ + *ERG6* strains were plated on YPD agar and incubated at different temperatures. The *erg*6Δ mutant displayed modestly reduced growth compared to the wild type at 25 and 30 °C. When the temperature was increased, the growth defect was more evident, as the mutant was thermo-sensitive at 35 °C and completely unable to grow at 37 °C (Fig. 4A). In order to analyze the thermo-sensitivity defect observed in the *erg*6Δ mutant, the strains were cultivated in 96-well plates in YPD and YNB, and the kinetics of growth were spectrophotometrically evaluated for 96 h at different temperatures (Fig. 4B). At 30 °C, all the strains had similar growth curves in YPD reaching stationary phase without statistically significant differences. While the wild type reached the plateau at 36 h, the *erg*6Δ took about 72 h (Fig. 4B). We observed a growth delay of *erg*6Δ strain in YNB, in which the mutant took 36 h to reach a lower plateau, as compared to the 24 h of the wild type. At 35 °C, the *erg*6Δ strain retardation in achieving stationary phase was more evident, with an extended exponential phase from 12 to 72 h, as compared to 12–36 h for the wild type. Finally, at 37 °C the *erg*6Δ strain was not able to grow, consistent with previous results on YPD agar plates (Fig. 4A). The reconstituted strain showed a growth profile similar to the wild type in all conditions tested. The absence of *ERG6* did not result in any morphological alteration in *C. neoformans* cells after growth on YPD agar plates at 30 °C. However, we observed that *erg*6Δ cells formed clusters after overnight growth at 30 °C in liquid YPD medium (Fig. S3 white arrow). We did not observe any pronounced effects on cell morphology after incubating

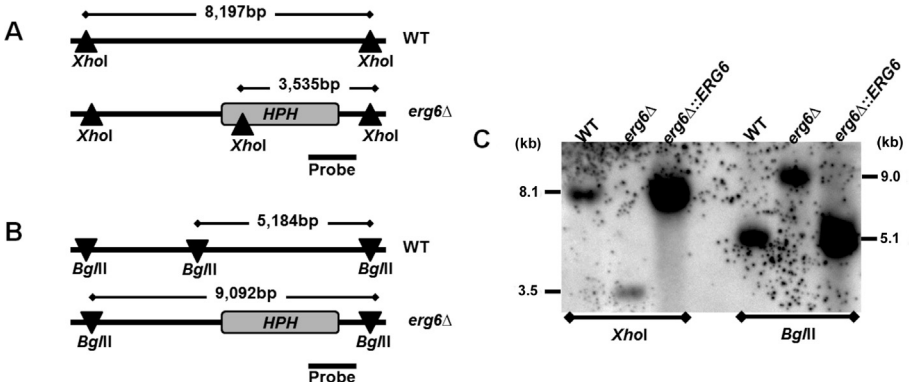

Fig. 2. Confirmation of the *ERG6* deletion and genetic reconstitution by Southern Blotting. XhoI (A) and BglII (B) restriction pattern of *ERG6* locus in the wild type and mutant. (C) Southern blotting of the genomic DNA of the strains: wild type, *erg*6Δ, and *erg*6Δ + *ERG6* digested with restriction enzymes XhoI and BglII probed with a 1099 bp DIG-labeled PCR fragment. The annealing region of the probe is indicated as a solid line. The positions of the XhoI and BglII restriction sites are represented by ▲ and ▼, respectively.

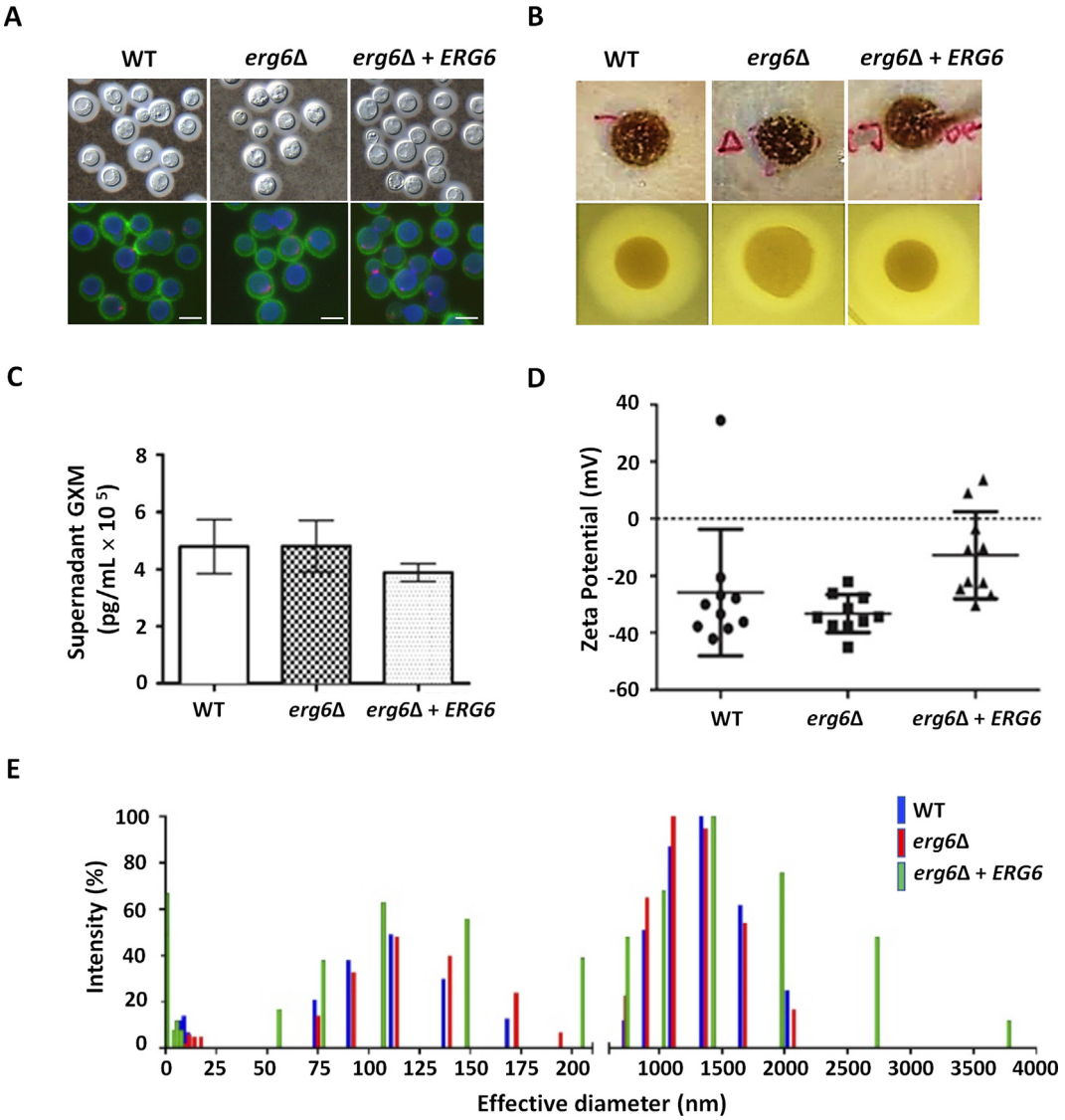

Fig. 3. *ERG6* deletion does not drastically affect *C. neoformans* main virulence traits. (A) Polysaccharide capsule was induced in liquid minimum medium for 48 h at 30 °C and visualized microscopically with India ink counterstain (upper panel). The strains were stained for GXM, chitin and chitooligomers using respectively: mAb 18B7 and a secondary FITC-labeled goat anti-mouse IgG (Fc specific) antibody (green), calcofluor white (blue), Alexa Fluor 594 conjugate of WGA (pink) (bottom panel). No difference in the capsule diameter was detected among the strains. Images were acquired in an Axioplan 2 (Zeiss, Germany) fluorescence microscope using a Color View SX digital camera and processed with the software system analySIS. (B) The melanin was induced in L-DOPA agar plates at 30 °C (upper panel). Phospholipase secretion was analyzed in an egg emulsion medium for 48 h in a 10^7 dilution at 35 °C (bottom panel). The decrease of the halo diameter in the mutant plate indicates a defect in the secretion of the enzyme. The Pz values for wild type, reconstituted and mutant strains are 0.52, 0.47 and 0.73, respectively. (C) Secreted GXM was quantified by ELISA. One Way Anova detected no statistical differences of samples (D) Analyses of Zeta potential of capsule fibers were similar. (E) Hydrodynamic size distribution of GXM fibers of the mutant, wild type and reconstituted was determined by dynamic light scattering. (For interpretation of the references to color in this figure legend, the reader is referred to the web version of this article.)

the wild type and *erg*6Δ mutant at 37 °C for 4 and 16 h. We found among both the mutant and the wild type cells a small proportion of cells with a rough, granular cellular surface and cytoplasm retraction (Fig. S3 black arrows). Other morphological defects in cell size or shape were not observed in *erg*6Δ mutant when compared to wild type strain. Our data corroborate the previous description of *erg* mutants (Toh-e et al., 2017) and emphasize the important role of Erg6 in the growth of *C. neoformans* at high temperatures.

3.5. Ergosterol content is decreased in the erg6Δ mutant

To determine if *erg*6Δ strain has altered sterol composition in the plasma membrane, we extracted fungal lipids by organic solvents solubility and evaluated their ergosterol content by HPLC. An ergosterol peak was detected at 281 nm after almost five minutes of retention, while lanosterol was detected at 220 nm after nearly 5.5 min. In this assay, *erg*6Δ strain did not show any detectable ergosterol, but lanosterol was identified as a peak at 220 nm (Fig. 5A). The amount of ergosterol in *erg*6Δ mutant was below the detection limit of the quantification method (0.1 μg/mg of total lipids), while lanosterol was estimated at about 11.7 μg/mg of total lipids. Interestingly, the *ERG6* deletion caused accumulation of an unidentified intermediate sterol detected as a high peak at 281 nm eluted with a retention time of approximately 4.4 min (Fig. 5A). The wild type and reconstituted strains had a similar pattern of sterols with the ergosterol peak after 5 min at 281 nm, with estimated amount of 4.21 and 7.62 μg/mg of total sterols, respectively, while lanosterol was not detected (Fig. 5B and C). Our data clearly demonstrated an inverse correlation between lanosterol

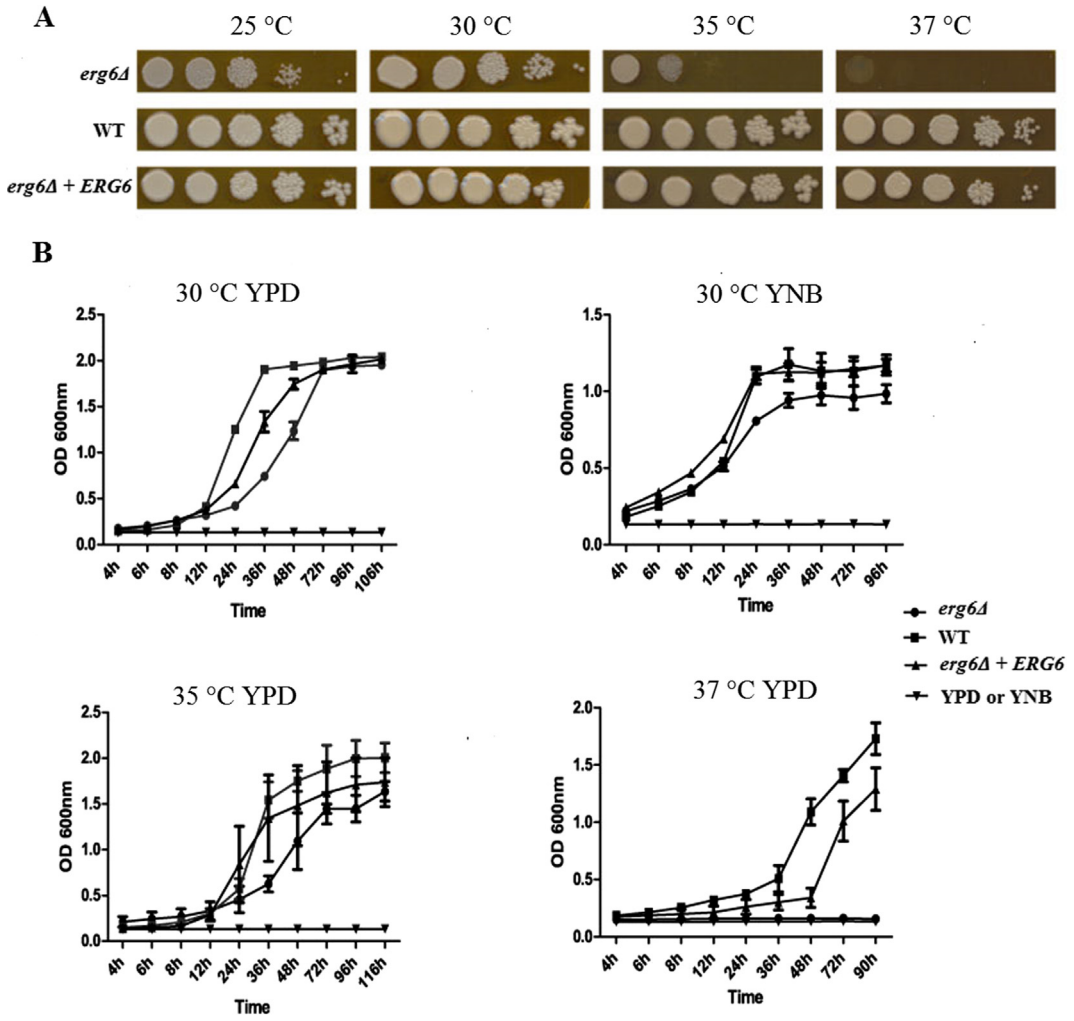

Fig. 4. *erg*6Δ has a growth defect at high temperature. (A) The *erg*6Δ, wild type and *erg*6Δ + *ERG6* strains were serially diluted on YPD plates and incubated at indicated temperatures. Growth was assessed after four days. Three independent experiments were performed in duplicate. (B) Growth curves of *erg*6Δ, wild type and *erg*6Δ + *ERG6* strains in liquid medium (YPD and YNB) at different temperatures. Optical densities at 600 nm were used to measure the growth of the cultures, every 30 min; the negative control was the medium without cells. All the cultures started with 10^6 cells per well in a 96-well plate, and each strain was inoculated in triplicate. (■) wild type, (●) *erg*6Δ, (▲) *erg*6Δ + *ERG6,* (▼) YPD or YNB without cells.

and ergosterol in which the wild type and reconstituted strains had undetectable lanosterol and increased ergosterol, whereas the mutant had the opposite pattern of membrane sterol composition.

3.6. *ERG6* deletion affects extracellular vesicles of *C. neoformans*

To identify if the *erg*6Δ strain produces extracellular vesicles, even in the absence of ergosterol, we cultivated the three strains *erg*6Δ, wild type and *erg*6Δ + *ERG6* on agar plates and proceeded to isolate EVs as described by (Reis et al., 2019). After removing of GXM from the extracted samples, we performed protein and sterol quantification. We observed an increased protein content on the EVs obtained from the mutant in relation to the wild type (P = 0.0043) and reconstituted strains (P = 0.0054) (Fig. 6A). Furthermore, the total sterol quantification showed that *erg*6Δ mutant produced significantly higher amount than wild type (P = 0.0017) and *erg*6Δ + *ERG6* strains (P = 0.0017) (Fig. 6B). Those data corroborate our sterol analysis by HPLC of the *erg*6Δ mutant (Fig. 5), in which we observed an increased amount of lanosterol and an unidentified intermediate sterol detected at 281 nm. Together, both analyses suggest the mutant compensates the absence of ergosterol, producing other types of sterol molecules. To confirm if *erg*6Δ mutant can produce EVs similarly to the wild type strain, we evaluated the hydrodynamic diameter distribution of EVs using DLS. According to Fig. 6C we observed a different distribution profile of vesicular diameters among the strains. The *erg*6Δ mutant presented a proportion of 79% of EVs with a diameter of 613.2 nm and 20.8% with an average diameter of 99.06 nm, with a polydispersity index (Pdi) of 0.526, indicating a heterogeneous distribution within the EVs suspension. In contrast, the wild type strain produced EVs with a more homogeneous suspension represented by a single peak on DLS analysis containing about 97.2% of EVs with an average diameter of 113.5 nm and a Pdi of 0.227, what indicates a lower dispersion of EVs in comparison to those produced by the mutant. The EVs of reconstituted strain also presented a low polydispersity feature (Pdi of 0.298) and most of the EVs (94.1%) had an average diameter of 255.8 nm. Our approach did not allow the morphological characterization of the vesicles, nor the identification of their cargo. However, these data suggest the absence of *ERG6* affects the production of EVs. These results open new perspectives for studying the role of ergosterol in the biogenesis and function of EVs, which are important regulatory components required for fungal communication and adaptation to the host and environment (de Toledo Martins et al., 2018; Rodrigues et al., 2008, 2007; Vargas et al., 2015).

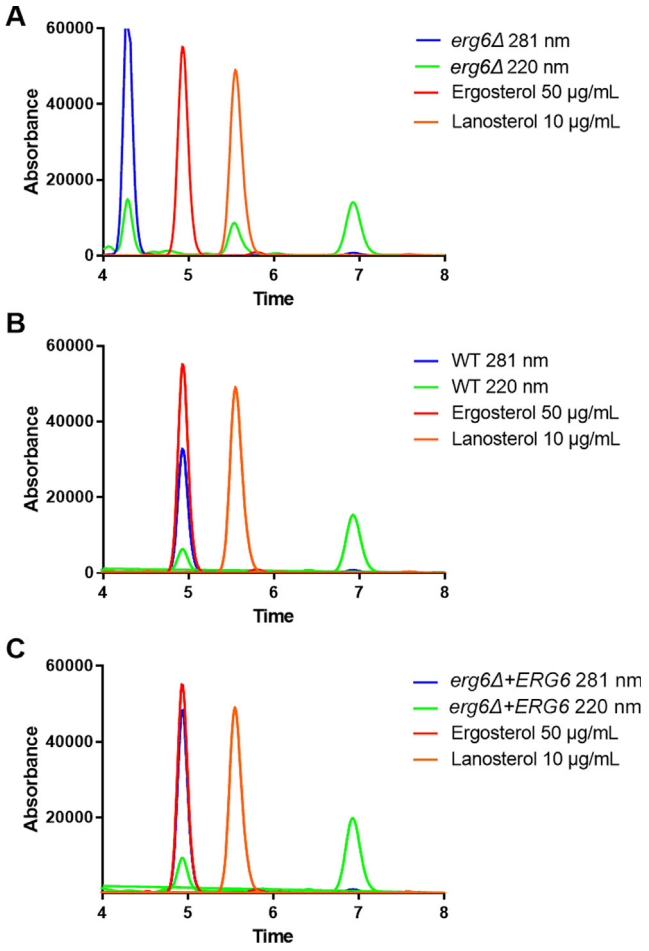

Fig. 5. HPLC analyses of total lipids extracted from *erg*6Δ, wild type and *erg*6Δ + *ERG6* strains. Lanosterol and ergosterol were the standard controls. After five minutes of elution, the ergosterol peak was visualized at 281 nm, and lanosterol appeared after 5.5 min at 220 nm. (A) The total lipids profile of *erg*6Δ was distinct from wild type. One sterol peak is observed between four and five minutes, not detected in the wild type and reconstituted strains. The *erg*6Δ ergosterol level was below the detection limit of the quantification method (0.1 µg/mg of total lipids), while lanosterol accumulated only in the mutant (11.7 µg/mg of total lipids). (B) and (C) Wild type and reconstituted strains respectively exhibited very similar lipids profile. The ergosterol content was estimated at 4.21 and 7.62 µg/mg of total lipids, for wild type and reconstituted strains, respectively, and lanosterol level was below the limit detected by the instrument for both strains. The color of the lines represents blue (ergosterol detection at 281 nm), green (lanosterol at 220 nm), red (standard: 50 µg/mL of ergosterol at 281 nm) and orange red (standard: 10 µg/mL of lanosterol at 220 nm). (For interpretation of the references to color in this figure legend, the reader is referred to the web version of this article.)

3.7. *erg6Δ mutant is severely affected by different stress conditions*

Previous work exploring *erg* mutants in *C. albicans* reported increased susceptibility to different stressors (Luna-Tapia et al., 2015) such as osmotic and oxidative agents and compounds that alter cell wall assembly. We tested if the *C. neoformans erg*6Δ mutant would display similar stress intolerance. As expected for strains with depleted ergosterol, *erg*6Δ mutant was unable to grow in high osmolarity conditions, such as 1.5 M of KCl and NaCl at 30 °C (Fig. 7). This phenotype of osmolarity susceptibility was previously demonstrated (Toh-e et al., 2017). We also observed a growth impairment of *erg*6Δ mutant in the presence of 0.05% SDS as well as on the cell wall disturbing agents Congo Red (0.5 and 1%) and caffeine (0.5 and 1 mg/mL) (Fig. 7). *erg*6Δ strain did not demonstrate altered susceptibility to the chitin binding anionic dye Calcofluor White (0.5 and 1 mg/mL) when compared to the wild type or reconstituted strains (Fig. 7).

The oxidative stress response of the *erg*6Δ strain was also evaluated after plating serial dilutions of the strains in YPD agar supplemented by 1 and 5 mM hydrogen peroxide. (Fig. 7). At the lowest concentration, all the strains grew after three days at 30 °C, but at the highest concentration tested, the mutant exhibited an inability to detoxify H_2O_2. This observation suggests that ergosterol plays an important role in the plasma membrane response to H_2O_2.

3.8. *erg6Δ strain is susceptible to several antifungal compounds*

Antifungal susceptibility was assessed by serial dilutions of the strains spotted on YPD agar containing different antifungal drugs, and the MICs were determined according to CLSI M27-A3 microdilution protocol. Several concentrations of the polyene AmB (0.5–8 µg/mL) were added to YPD agar plates, the *erg*6Δ strain demonstrated enhanced AmB resistance (Fig. 8B). The AmB MIC of the mutant was four-fold higher (2 µg/mL), when compared to the wild type and reconstituted strains (0.5 µg/mL) (Table 1), similar to previous report (Toh-e et al., 2017). Similarly, the *erg*6Δ mutant demonstrated relative tolerance to nystatin, both by agar-based assay and MIC testing (Fig. 8A, Table 1). This effect was also observed in ascomycetes as *C. albicans* and *S. cerevisiae* (Gaber et al., 1989; Jensen-Pergakes et al., 1998). The increased resistance to polyenes is expected due to the diminished content of ergosterol in *C. neoformans erg*6Δ mutant (Fig. 5), as this molecule is the target of those antifungal molecules. This relationship between polyene resistance, azole sensitivity, and sterol composition (ergosterol depletion) was previously verified for others *C. neoformans erg* mutants (Kim et al., 1975), and in *C. albicans, C. tropicalis, C. glabrata* and *C. neoformans* clinical isolates (Kelly et al., 1994; Vandeputte et al., 2007; Vincent et al., 2013). Usually AmB resistance is rarely found among clinical isolates (Pfaller et al., 2005), as ergosterol depletion causes drastic consequences for the fungal cells that affect homeostasis and virulence.

The *erg*6Δ strain had an increased susceptibility to several azoles such as itraconazole, fluconazole and ketoconazole (Fig. 8A). The MICs for wild type were, respectively, 0.125 µg/mL, 4 µg/mL and 2 µg/mL for ketoconazole, fluconazole and itraconazole (Table 1). However, the *erg*6Δ mutant did not grow even at the lower concentration (0.03 µg/mL) of these drugs. Increased susceptibility of the *erg*6Δ mutant was also observed for terbinafine, a drug from the allylamine class that blocks squalene 2,3-epoxidase (Erg1), an early enzyme of ergosterol biosynthesis (Fig. 8A). The MIC for the mutant was two-fold reduced as compared to the wild type (Table 1). Together these results strongly suggest a synergistic effect of the inhibition of Erg6 and Erg11 two enzymes in the same pathway, reinforcing the potential of Erg6 as a powerful target for the development of new antifungal compounds.

The *erg*6Δ strain was not able to grow at 1.0 µg/mL of cerulenin, an antibiotic that irreversibly inactivates the yeast fatty acid synthetase; the MIC was 0.25 µg/mL for the mutant and 0.5 µg/mL for wild type and reconstituted strain (Fig. 8A; Table 1). In *C. albicans*, the *erg*6Δ mutant susceptibility was two-fold increase in comparison to wild type (Jensen-Pergakes et al., 1998).

Two other drugs were used to evaluate the *erg*6Δ strain: brefeldin A, an antibiotic that prevents protein-vesicle transport, and FK506, which targets the calcineurin signaling pathway (Fig. 8A). In the agar plates assay, the mutant was slightly sensitive to brefeldin A (32 µg/mL), and the MIC of the *erg*6Δ strain decreased four-fold, when compared to the other strains (Table 1). Interestingly, in *C. albicans,* the brefeldin A MIC for the *erg*6Δ mutant had a 50-fold reduction in comparison to the wild type (Jensen-Pergakes et al., 1998). The results obtained from both pathogens indicate that the changes in ergosterol content of yeast cells may affect other cellular processes in addition to sterol synthesis (Table 1). Regarding FK506, the MIC of *erg*6Δ strain was 0.06 µg/mL while for wild type and reconstituted strains it was 0.25 µg/mL. In addition, mutant growth was completely abolished on agar plates

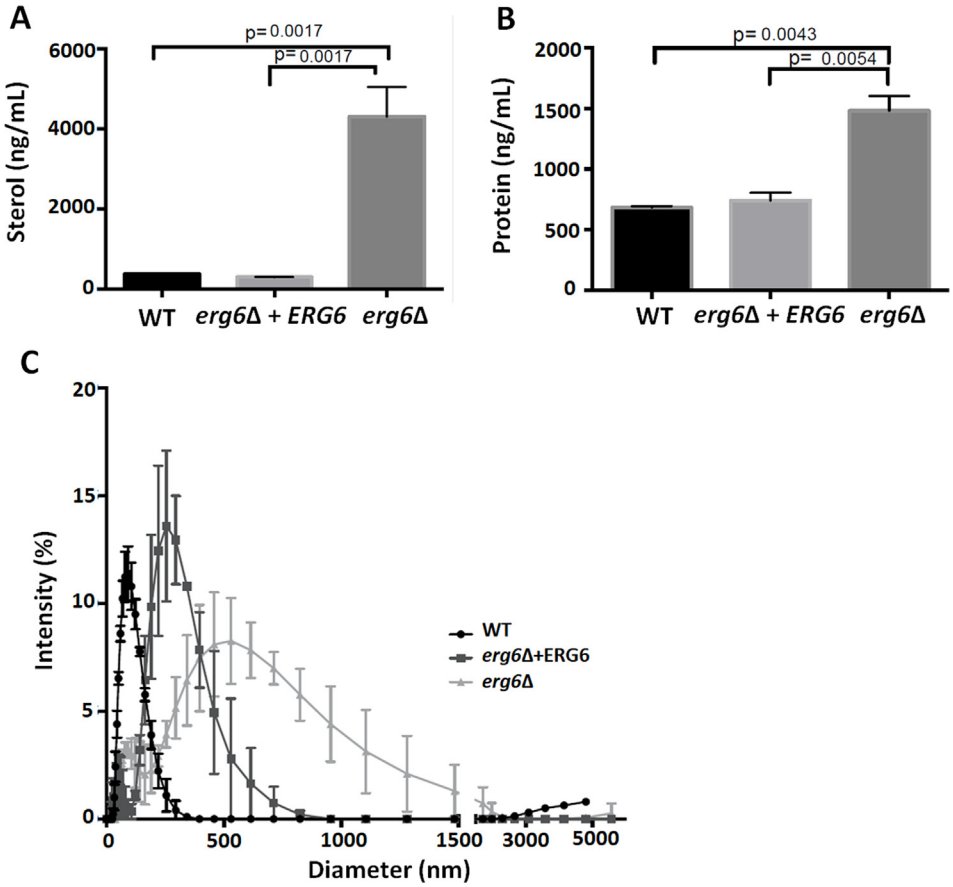

Fig. 6. Erg6 affects extracellular vesicle properties. EVs were harvest from individual *C. neoformans* strains and total sterol (A) and protein (B) content were quantified using colorimetric assays: Amplex Red Cholesterol assay kit and Micro BCA Protein assay kit, respectively. The graphics are representative of at least three independent assay. One Way Anova was used to assess statistical significance ($P < 0.05$ is indicated). (C) Hydrodynamic diameter distribution in percentage of EVs isolated from *C. neoformans* H99, *erg6*Δ and reconstituted strains using Dynamic Light Scattering (DLS). The graphic is representative of two different experiments.

containing 1 μg/mL of FK-506.

3.9. *erg6Δ strain is avirulent in a wax moth model*

Using macrophage phagocytosis assay after co-cultivation of J774 macrophages and *C. neoformans,* we found phagocytosis rate was comparable among strains: 90% for H99 (227/251 macrophages containing yeast), 88% for *erg6* (237/270) and 82% for *erg6*Δ + *ERG6* (306/369) (Fig. S4B). However, *erg6*Δ cells demonstrated a statistical significantly reduced survival rate when compared to the wild type and the reconstituted strains (Fig. S4). This result is quite expected for a temperature sensitive strain due to its inability to proliferate under this condition. For this reason, we decided to use the *G. mellonella* invertebrate animal model to investigate the *in vivo* virulence of the *erg6*Δ mutant at two different temperatures of incubation, 30 and 37 °C. After inoculation, the larvae were daily observed for mortality. At 30 °C (Fig. 9A) and 37 °C (Fig. 9B) the *erg6*Δ mutant was less virulent relative to wild type ($P < 0.0001$) and the reconstituted strains ($P < 0.0001$). At both temperatures, we did not observe altered mortality between the group infected with *erg6*Δ strain and the control inoculated with PBS ($P > 0.29$). In contrast, all larvae in the groups infected with the wild type or reconstituted strain died on the 9th (30 °C) and 5th (37 °C) day after inoculation. The loss of virulence cannot be attributed exclusively to the temperature sensitivity of the mutant.

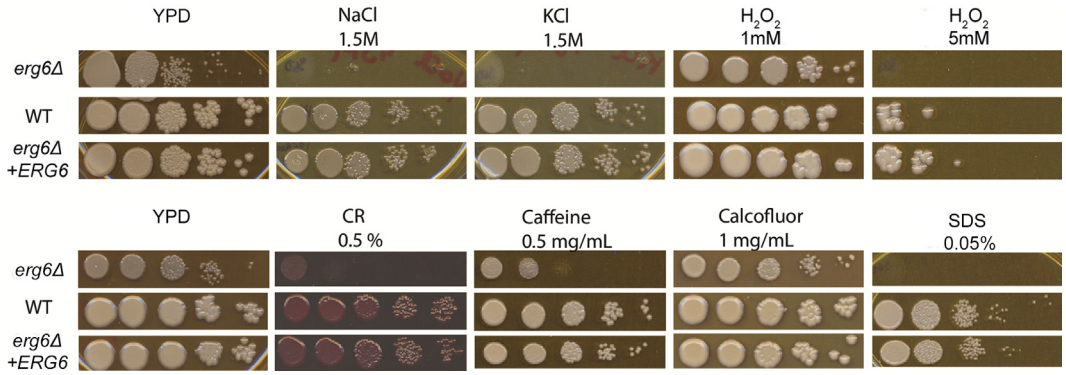

Fig. 7. *C. neoformans erg6*Δ mutant is sensitive to osmotic, oxidative and cell wall stress conditions. Yeast cells were serially diluted from 10^7 to 10^3 cells/mL, plated on YPD agar with different stress agents, and incubated at 30 °C until the colonies appeared. Osmotic stress response was assessed with 1.5 M of NaCl and KCl. Oxidative stress tolerance was tested with 1 and 5 mM H_2O_2. The cell wall stressor compounds were Congo Red (0.5%), caffeine (0.5 mg/mL), calcofluor White (1 mg/mL) and SDS (0.05%). Three independent experiments were performed in duplicate. (For interpretation of the references to color in this figure legend, the reader is referred to the web version of this article.)

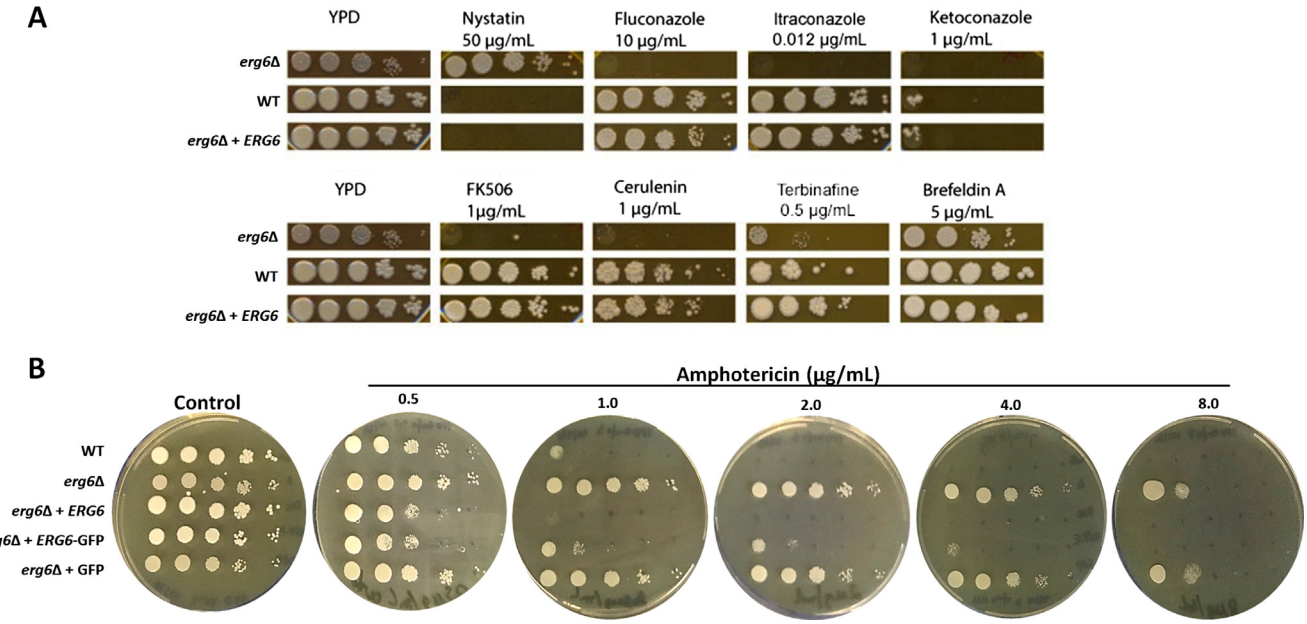

Fig. 8. Growth responses of the *erg*6Δ, wild type and *erg*6Δ + *ERG6* strains in the presence of 0.9% NaCl, serially diluted to 10^7 cells/mL, and 5 μL were plated on YPD agar supplemented with different drugs. The cells were incubated at 30 °C for seven days. (A) The concentrations tested were nystatin 50 μg/mL, fluconazole 10 μg/mL, itraconazole 0.012 μg/mL, ketoconazole 1 μg/mL, FK506 1 μg/mL, cerulenin 1 μg/mL, terbinafine 0.5 μg/mL and brefeldin A 5 μg/mL. (B) AmB susceptibility was evaluated using drug concentrations ranging from 0.5 to 8 μg/mL. The strains *erg*6Δ + *ERG6*-GFP and *erg*6Δ + GFP were also included on the test.

Table 1
MIC of the strains for several antifungal agents.

	MIC (μg/mL)		
	*erg*6Δ	WT	*erg*6Δ + *ERG6*
Amphothericin B	2	0.5	0.5
Nystatin	16	2	2
Fluconazole	< 0.03	4	4
Itraconazole	< 0.03	2	2
Ketoconazole	< 0.03	0.125	0.125
Terbinafine	0.25	0.5	0.5
Cerulenin	0.25	0.5	0.5
Brefeldin A	8	> 32	> 32
FK-506	0.03	0.25	0.25

3.10. Erg6 localizes in ER and Golgi apparatus of C. neoformans

We fused the *C. neoformans* Erg6 protein to GFP to access its cellular localization by fluorescence microscopy. Prior to the experiment, we confirmed that *ERG6*-GFP fusion partially restored the functionality of Erg6 as can be evidenced by the phenotypic rescue of *erg*6Δ + *ERG6*-GFP strain. This strain grew on liquid and solid YPD at 37 °C similarly to the wild type and reconstituted strains (Fig. S5). We also plated the strains on different concentrations of AmB, and the *erg*6Δ + *ERG6*-GFP rescued the susceptible phenotype of the wild type strain (Fig. 8B). We observed different patterns of GFP fluorescence, with discrete cytoplasmic structures (arrows in Fig. 10 and Fig. S6) or a more diffuse perinuclear distribution (arrowheads in Fig. S6). Using organelle fluorescent markers ER-tracker and BODIPY-ceramide, we found colocalization with the endoplasmic reticulum (ER) and Golgi complex (Fig. 10). Mitotracker, Calcofluor White and FM 4-64, which bind, respectively, the mitochondria, cell wall and vacuolar membranes, did not co-localize with Erg6-GFP (Fig. S5). This pattern of localization is consistent with the fact that sterols are typically synthesized in the ER (Daum et al., 1998), and after maturation the molecules are transported in a non-vesicular manner to the plasma membrane (Baumann et al., 2005; Jacquier and Schneiter, 2012; Lv et al., 2016).

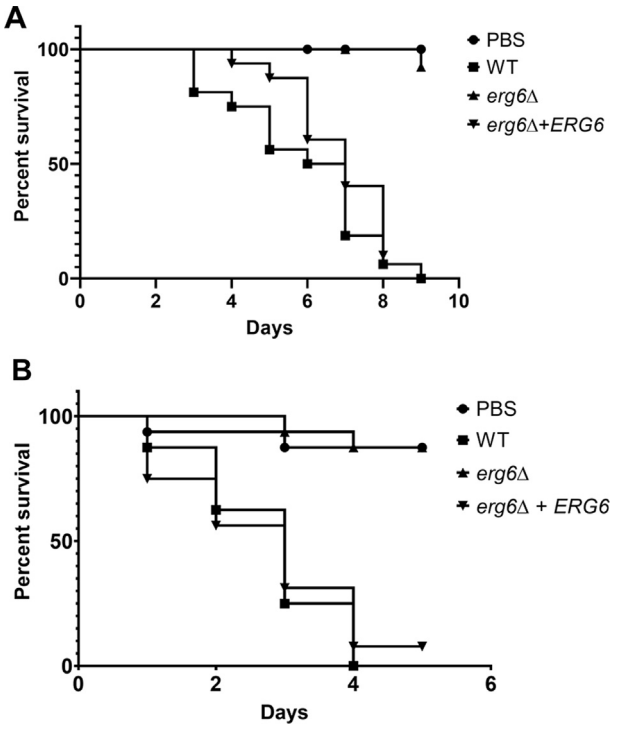

Fig. 9. The deletion of *ERG6* results in reduced virulence in *G. mellonella*. *G. mellonella* virulence assays were performed with an initial inoculum of 5×10^6 cells/caterpillar. n = 16 caterpillars for each strain. The infected caterpillars were observed every day until the last one died. The mutant strain was less virulent in this model at both temperatures tested, 30 °C (A) and 37 °C (B). Survival curves were analyzed using log-rank and Wilcoxon tests using Graphpad 8.0. Statistical significant differences and P values < 0.0001 were observed on the comparison of the groups WT × *erg*6Δ, *erg*6Δ × *erg*6Δ + *ERG6* for both temperatures analyzed.

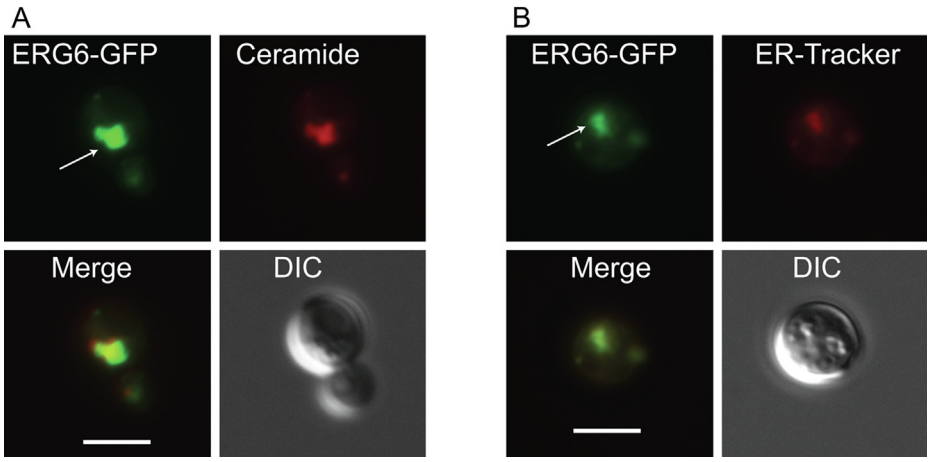

Fig. 10. Erg6-GFP fusion localizes intracellularly in Golgi apparatus and Endoplasmic Reticulum. Strains were grown in YPD medium overnight, washed in saline, and 10^6 cells were re-suspended in the dyes, according to description in the material and methods section. The cells were observed using an inverted microscope *Zeiss Axio Observer Z1* by differential interference contrast. Lens Plan-Apochromat 63×/1.40 Oil DIC M27. (A) Cells stained with Bodipy-Ceramide (5 μM, for 10 min at 4 °C) to assess co-localization with the Golgi complex. (B) Endoplasmic reticulum co-localization was assessed after incubation of the cells with ER-Tracker 10 μM for 20 min at 30 °C.

4. Discussion

Plasma membranes are formed by a combination of different lipids, sterol and proteins, that can combine in domains establishing its physical and chemical properties (Ermakova and Zuev, 2017). The presence of ergosterol in the membrane influences the structural organization that maintains its dynamic function as the cellular homeostasis (Alvarez et al., 2007).

Mutants defective in enzymes related to sterol biosynthesis have been used to study the ergosterol pathway and understanding the function of this unique molecule in fungal biology (Karst and Lacroute, 1974, 1973; Kim et al., 1975; Servouse and Karst, 1986). More recently, the appearance of azole-resistant strains supported the quest for more detailed information about how the ergosterol biosynthetic pathway is orchestrated and how ergosterol plays a structural and signaling role in different human fungal pathogens. Many ergosterol mutants have defective growth, such as *erg26* in *S. cerevisiae* (Gachotte et al., 1998), *erg24* in *C. albicans* (Jia et al., 2002), *erg6* in *C. lusitaniae* (Young et al., 2003), and others.

In this work, we evaluated the *erg6*Δ strain growth phenotype, the drug susceptibility profile and ergosterol content, as well as the mutant's ability to cause infection. *ERG6* is not an essential gene in *C. neoformans*, nor in the ascomycetes *S. cerevisiae, K. lactis* or *Candida* species (Gaber et al., 1989; Jensen-Pergakes et al., 1998; Konecna et al., 2016; Toh-e et al., 2017; Young et al., 2003); however, we show that the *C. neoformans* mutant has severe growth defects under high temperature and osmotic and oxidative stress conditions, and it has attenuated virulence in an invertebrate model of infection. In addition, by HPLC we detected unbalanced sterol content with reduced content of ergosterol and increased lanosterol, with an antifungal susceptibility pattern different from the wild type strain resulting in resistance to polyenes and hypersensitivity to azoles.

Nes et al. 2009 described the sterol profile in *C. neoformans* and identified that 39% of total sterols were ergosterol, while only 3% were lanosterol. Those authors, using CG-MS sterol analysis, also showed accumulation of intermediate sterols (lanosterol, eburicol and 32-nor-eburicol) when *C. neoformans* yeast cells were treated with Erg6 inhibitors. Our data are in accordance with previous work (Vandeputte et al., 2007; Young et al., 2003) that reported a decreased ergosterol content and an altered sterol membrane composition in *erg6* mutants of *C. glabrata* and *C. lusitaniae*, respectively. *ERG6* deletion resulted in ergosterol depletion in membrane composition, thus contributing to the growth defect observed in the mutant.

Among the features shared by many *erg* mutants, the incapacity to grow under high osmolality conditions is of great importance. In accordance with Toh-e and colleagues (Toh-e et al., 2017), we also observed *C. neoformans erg6*Δ mutant was unable to grow in high concentration of NaCl, KCl and sorbitol. Many reports highlight the role of ergosterol on membranes properties, such as fluidity, permeability, microdomain formation, protein transport and functionality (Ermakova and Zuev, 2017; Hu et al., 2017; Iwaki et al., 2008; Zhang and Rao, 2010). The nature of the membrane sterol content is crucial for the cell to respond to environmental stress. Dupont et al. (Dupont et al., 2011) studied the relationship of membrane sterols and resistance of *S. cerevisiae* to osmotic stressors, and they observed *erg6* mutants accumulate ergosterol precursors and are more susceptible to osmotic variations compared to wild type. Ergosterol molecules promote an increased mechanical resistance of the plasma membrane, like deformative capacity and resistance to stretching, important for cellular adaptation to hydric changes in the environment, in comparison to their precursors' roles in response to osmotic and oxidative stress. In fact, the distinctive sterol profile that we observed in the *erg6*Δ strain (accumulation of lanosterol and other sterols not identified in our chromatograms) may be the reason for impaired growth under osmotic conditions reported here. Using 24-SMT inhibitors, Nes and others (Nes et al., 2009) also detected lanosterol accumulation in *C. neoformans* yeast cells. The alteration in membrane sterols with accumulation of intermediate sterols was also detected after treatment of *Paracoccicioides brasiliensis* (Visbal et al., 2011), *S. schenckii* and *S. brasiliensis* (Borba-Santos et al., 2016) with Erg6 inhibitors.

To date, there are no reports that demonstrate the role of ergosterol in biogenesis and activity of EVs. Previous studies have detected ergosterol among the main lipid components of the *C. albicans* and *C. neoformans* EVs (Rodrigues et al., 2007; Vargas et al., 2015). Our data, demonstrate that the absence of *ERG6* generates vesicles with a higher polydispersity index and increased levels of proteins and sterols. Extracellular vesicles have been drawing attention over the last years and recent works point to an active role of these structures as carriers of several molecules that modulate the interaction of fungi with the environment (Albuquerque et al., 2008; Bielska and May 2019; Bitencourt et al., 2018; Ikeda et al., 2018; Rodrigues et al., 2008, 2007; Vallejo et al., 2012; Vargas et al., 2015; Zamith-Miranda et al., 2018). Immune modulation has been described after cells or animals are exposed to fungal EVs (Albuquerque et al., 2018; Baltazar et al., 2018; Bitencourt et al., 2018; Gehrmann et al., 2011; Oliveira et al., 2010; Vargas et al., 2015). In addition *C. neoformans* EVs can contribute to pathogenesis once they accumulate in sites of brain infection, promoting adhesion and transcytosis of yeasts in microvascular endothelial cells (Huang et al., 2012). Our results show that the absence of ergosterol in *C. neoformans* does not affect its capacity to produce EVs, indicating that the mutant strain likely uses other types of sterols to generate these structures. Microorganisms can modulate characteristics and composition of EVs depending on environmental circumstances (Brown et al., 2015), however the biological impact of the altered ergosterol content

of EVs in *C. neoformans erg6*Δ mutant is still a question to be answered.

We also observed increased sensitivity of *C. neoformans erg6*Δ mutant to high concentration of H_2O_2. Branco et al. (Branco et al., 2004) attributed this phenotype of yeast *erg6*Δ to enhanced membrane permeability, caused by absence of a H_2O_2 catalase- driven gradient in membranes in addition to altered fluidity (Branco et al., 2004; Folmer et al., 2008). Also, the high susceptibility of the *C. neoformans erg6*Δ strain to the cell wall stressors Congo Red and SDS possibly indicates that cell wall structure might be weakened or not properly anchored in the plasma membrane, favoring the entrance of exogenous compounds like the anionic detergent SDS. *C. glabrata erg6* mutants displayed a similar phenotype (Vandeputte et al., 2007). The stress-related growth defects of *erg6* mutants may also be a consequence of disturbances in surface of the cell caused possibly by altered protein trafficking or mislocation of cell wall-related enzymes. *ERG6* was identified as necessary for the trans-Golgi network transport of proteins (Proszynski et al., 2005). Membrane ergosterol is required for targeting to the cell surface several biologically important proteins involved in cations and pH homeostasis, nutrient, pheromones and virulence factors transport, drug efflux and stress response (Daum et al., 1998; Espenshade and Hughes, 2007; Kodedová and Sychrová, 2015; Umebayashi and Nakano, 2003).

Our data clearly demonstrated that the *C. neoformans erg6*Δ strain has major growth impairments at 37 °C and altered growth rates at 30 and 35 °C. As the ability to grow at high temperature is an intrinsic characteristic of a human pathogen, we hypothesized that *erg6*Δ mutant would demonstrate virulence defects. After macrophage phagocytosis, *erg6*Δ strain had reduced survival. Also, the mutant was avirulent at 37 °C and hypovirulent at 30 °C in the *Galleria* virulence model. These data suggest a pathogenicity defect caused not only by the incapacity to adapt to high temperature, but also to a more complex mechanism in which ergosterol is required for the host-pathogen interaction. Recently, Koselny et al. (Koselny et al., 2018) provided evidence that ergosterol is recognized by immune cells, and highlighted this is not only a structural molecule, but it has an active role in the host-pathogen interaction. They demonstrated a close relationship between the amount of ergosterol and the capacity of yeast cells to induce macrophage lysis by pyroptosis. Kim et al. (Kim et al., 1975) isolated six *C. neoformans* UV-irradiated mutants resistant to polyenes with attenuation of virulence in mice and growth reduction dependent on temperature. Jia et al., (Jia et al., 2002) also reported a slow growth under several conditions and reduced mortality of mice infected with *erg24* mutants of *C. albicans*.

In this work, we observed the antifungal susceptibility profile for *erg6*Δ mutant was significantly altered from the wild type strain. We tested several commercially available antifungal drugs and metabolic inhibitors, and we found *erg6*Δ mutant is extremely susceptible to azoles and allylamines, whereas it demonstrated relative resistance to polyenes. The synergism between *ERG6* deletion and inhibition of Erg11 by azoles has a wide applicability for future development of new molecules that are able to target Erg6. The use of drugs affecting two enzymes of the same ergosterol cascade points to a possible reduction in dosages and consequently fewer side effects for the patients. In addition, a well-known advantage of combination therapy is that the emergence of resistance to two concomitant antimicrobials would be impaired. Because of the effect on the cellular membrane, the combination of Erg6 inhibitors and other drugs with different mechanism of action could be a clinical strategy to favor the enhanced uptake of drugs. Other compounds such as FK-506, cerulenin and brefeldin A, also had a strong inhibitory effect on *erg6*Δ. Previous studies confirm that the calcineurin pathway plays a role in the membrane stress survival pathway of fungi and the synergism of FK-506 and members of the azole class exhibited strong activity against susceptible and resistant strains of *C. albicans* (Chen et al., 2013; Cruz and Goldstein, 2002; Onyewu et al., 2003).

The multiple alterations in antifungal drug susceptibility in *erg6*Δ mutant point to a greater need for understanding the role of ergosterol in the development of resistance to the azoles and polyenes, the most commonly used agents in clinical treatments against fungal infections. Antimicrobial resistance is a complex trait generated by a combination of several mechanisms. The evolved mechanisms include alteration of ergosterol biosynthesis components by genetic mutations (for example *ERG11*, *ERG2*, *ERG3*), regulation of transcriptional factors related to sterol response *UPC2* in *C. albicans* (Flowers et al., 2012; Silver et al., 2004) and *SRE1* in *C. neoformans* (Chang et al., 2009); expression of efflux pump transporters (Vincent et al., 2013; White, 1997), activation of stress responsive signal transduction pathways (HOG1) (Ko et al., 2009), PKC (Lafayette et al., 2010), Calcineurin and HSP90 (Cowen and Lindquist, 2005; Cowen and Steinbach, 2008; Cruz and Goldstein, 2002); and others (Robbins et al., 2017; Xie et al., 2014). The resistance to AmB and increased susceptibility to azoles caused by ergosterol depletion observed in *erg6* mutants may be one of many mechanisms the fungal cells have evolved to respond to drugs. Clinical isolates of *C. glabrata* resistant to AmB had reduction of ergosterol content caused by missense mutations in the *ERG6* gene (Vandeputte et al., 2007), while *C. neoformans* with defective sterol delta 8–7 isomerase shares the same phenotype (Kelly et al., 1994). One *C. albicans* strain resistant to both AmB and azoles was demonstrated to have an altered membrane lipid composition with reduction of ergosterol and accumulation of a methylated sterol as a common basis for the double resistance (Hitchcock et al., 1987). In contrast, some *C. neoformans* clinical isolates resistant to AmB did not demonstrate a reduction of ergosterol levels (Joseph-Horne et al., 1996). Thus, given the complexity of this topic, future studies focusing on the modulation of ergosterol and its real impact in the resistance emergence scenario may clarify the mechanisms adopted by fungal pathogens to counteract polyenes and azoles effect. This knowledge will lead to new approaches to deal with the appearance of resistant clinical isolates, assisting in monitoring the susceptibility profiles to antifungal drugs and improve the efficacy of the most common drugs used in clinical treatment of those infections.

The detailed knowledge about ergosterol biosynthetic pathways and their regulation will encourage the identification of new molecular targets for the development of antifungal drugs and/or may be useful to modulate the immune response against the pathogens. The deletion of *ERG6* in *C. neoformans* demonstrated that absence of the enzyme affects many cellular processes, including pathogenicity, indicating that an inhibitor of this protein has great potential to treat cryptococcosis and other fungal diseases. The data generated by this work reinforces the multiple roles of ergosterol as an active and dynamic molecule on the surface of several fungal species, from ascomycetes to basidiomycetes. Our findings also contribute to the response to the last decade's global demand for the identification of new molecular targets with potential for treating fungal diseases that affect humans.

Credit authorship contribution statement

Fabiana Freire M. Oliveira: Formal analysis, Investigation, Writing - original draft. **Hugo Costa Paes:** Methodology, Investigation, Writing - review & editing. **Luísa Defranco F. Peconick:** Investigation. **Fernanda L. Fonseca:** Formal analysis, Investigation, Writing - review & editing. **Clara Luna Freitas Marina:** Formal analysis, Investigation, Writing - review & editing. **Anamélia Lorenzetti Bocca:** Methodology, Resources, Funding acquisition. **Mauricio Homem-de-Mello:** Methodology, Formal analysis, Investigation, Resources. **Márcio Lourenço Rodrigues:** Methodology, Resources, Funding acquisition. **Patrícia Albuquerque:** Methodology, Formal analysis, Investigation, Writing - review & editing. **André Moraes Nicola:** Methodology, Formal analysis, Investigation, Writing - review & editing. **J. Andrew Alspaugh:** Conceptualization, Writing - review & editing, Funding acquisition. **Maria Sueli S. Felipe:** Conceptualization, Resources, Supervision, Project administration, Funding acquisition. **Larissa Fernandes:** Conceptualization, Investigation, Resources, Writing -

original draft, Writing - review & editing, Visualization, Supervision, Project administration, Funding acquisition.

Acknowledgments

We thank Dr. Susana Frases for help with DLS and zeta potential measurements. This work was sponsored by the Conselho Nacional de Desenvolvimento Científico e Tecnológico, Brazil (CNPq) Grant (GENOPROT 559572/2009-3) and Fundação de Apoio à Pesquida do Distrito Federal, Brazil (FAP-DF) (PRONEX 193.000.569/2009 and 193.001.533/2016) to MSSF and Coordenação de Aperfeiçoamento de Pessoal de Nível Superior, Brazil (CAPES). JAA is supported by a National Institutes of Health, United States (NIH) grant R01 AI074677. M.L.R. is currently on leave from the position of Associate Professor at the Microbiology Institute of the Federal University of Rio de Janeiro, Brazil. M.L.R. was supported by grants from the Brazilian Ministry of Health, Brazil (440015/2018-9), Conselho Nacional de Desenvolvimento Científico e Tecnológico, Brazil (CNPq) 405520/2018-2, and 301304/2017-3) and Fiocruz, Brazil (VPPCB-007- FIO-18 and VPPIS-001-FIO18). The authors also acknowledge support from the Instituto Nacional de Ciência e Tecnologia de Inovação em Doenças de Populações Negligenciadas, Brazil (INCT-IDPN).

Appendix A. Supplementary material

Supplementary data to this article can be found online at https://doi.org/10.1016/j.fgb.2020.103368.

References

Albuquerque, P.C., Nakayasu, E.S., Rodrigues, M.L., Casadevall, A., Zancope-oliveira, R.M., Almeida, I.C., Baltazar, L.M., Zamith-Miranda, D., Burnet, M.C., Choi, H., Nimrichter, L., Nakayasu, E.S., Nosanchuk, J.D., Bielska, E., May, R.C., Bitencourt, T.A., Rezende, C.P., Quaresemin, N.R., Moreno, P., Hatanaka, O., Rossi, A., Martinez-Rossi, N.M., Almeida, F., Brown, L., Wolf, J.M., Prados-Rosales, R., Casadevall, A., Cowen, L.E., Lindquist, S., Steinbach, W.J., Flowers, S.A., Barker, K.S., Berkow, E.L., Toner, G., Chadwick, S.G., Gygax, S.E., Morschhäuser, J., David Rogers, P., Gehrmann, U., Qazi, K.R., Johansson, C., Hultenby, K., Karlsson, M., Lundeberg, L., Gabrielsson, S., Scheynius, A., Hitchcock, C.A., Barrett-Bee, K.J., Russell, N.J., Huang, S.H., Wu, C.H., Chang, Y.C., Kwon-Chung, K.J., Brown, R.J., Jong, A., Ikeda, M.A.K., De Almeida, J.R.F., Jannuzzi, G.P., Cronemberger-Andrade, A., Torrecilhas, A.C.T., Moretti, N.S., Da Cunha, J.P.C., De Almeida, S.R., Ferreira, K.S., Kelly, S.L., Lamb, D.C., Taylor, M., Corran, A.J., Baldwin, B.C., Powderly, W.G., Ko, Y.J., Yu, Y.M., Kim, G.B., Lee, G.W., Maeng, P.J., Kim, S., Floyd, A., Heitman, J., Bahn, Y.S., Lafayette, S.L., Collins, C., Zaas, A.K., Schell, W.A., Betancourt-Quiroz, M., Leslie Gunatilaka, A.A., Perfect, J.R., Cowen, L.E., Oliveira, D.L., Freire-de-Lima, C.G., Nosanchuk, J.D., Casadevall, A., Rodrigues, M.L., Nimrichter, L., Pfaller, M.A., Messer, S.A., Boyken, L., Rice, C., Tendolkar, S., Hollis, R.J., Doern, G.V., Diekema, D.J., Reis, F.C.G., Borges, B.S., Jozefowicz, L.J., Sena, B.A.G., Garcia, A.W.A., Medeiros, L.C., Martins, S.T., Honorato, L., Schrank, A., Vainstein, M.H., Kmetzsch, L., Nimrichter, L., Alves, L.R., Staats, C.C., Rodrigues, M.L., Silver, P.M., Oliver, B.G., White, T.C., Vincent, B.M., Lancaster, A.K., Scherz-Shouval, R., Whitesell, L., Lindquist, S., Westman, J., Hube, B., Fairn, G.D., White, T.C., Zamith-Miranda, D., Nimrichter, L., Rodrigues, M.L., Nosanchuk, J.D., 2018. Role of Candida albicans transcription factor Upc2p in drug resistance and sterol metabolism. Eukaryot. Cell 11, 1–10. https://doi.org/10.1111/cmi.13016.

Albuquerque, P.C., Nakayasu, E.S., Rodrigues, M.L., Frases, S., Casadevall, A., Zancope-Oliveira, R.M., Almeida, I.C., Nosanchuk, J.D., 2008. Vesicular transport in Histoplasma capsulatum: an effective mechanism for trans-cell wall transfer of proteins and lipids in ascomycetes. Cell. Microbiol. 10, 1695–1710. https://doi.org/10.1111/j.1462-5822.2008.01160.x.

Alcazar-Fuoli, L., Mellado, E., Garcia-Effron, G., Lopez, J.F., Grimalt, J.O., Cuenca-Estrella, J.M., Rodriguez-Tudela, J.L., 2008. Ergosterol biosynthesis pathway in Aspergillus fumigatus. Steroids 73, 339–347. https://doi.org/10.1016/j.steroids.2007.11.005.

Alvarez, F.J., Douglas, L.M., Konopka, J.B., 2007. Sterol-rich plasma membrane domains in fungi. Eukaryot. Cell 6, 755–763. https://doi.org/10.1128/EC.00008-07.

Baltazar, L.M., Zamith-Miranda, D., Burnet, M.C., Choi, H., Nimrichter, L., Nakayasu, E.S., Nosanchuk, J.D., 2018. Concentration-dependent protein loading of extracellular vesicles released by Histoplasma capsulatum after antibody treatment and its modulatory action upon macrophages. Sci. Rep. 8, 1–10. https://doi.org/10.1038/s41598-018-25665-5.

Baumann, N.A., Sullivan, D.P., Ohvo-Rekilä, H., Simonot, C., Pottekat, A., Klaassen, Z., Beh, C.T., Menon, A.K., 2005. Transport of newly synthesized sterol to the sterol-enriched plasma membrane occurs via nonvesicular equilibration. Biochemistry 44, 5816–5826. https://doi.org/10.1021/bi048296z.

Bielska, E., May, R.C., 2019. Extracellular vesicles of human pathogenic fungi. Curr. Opin. Microbiol. 52, 90–99. https://doi.org/10.1016/j.mib.2019.05.007.

Bitencourt, T.A., Rezende, C.P., Quaresemin, N.R., Moreno, P., Hatanaka, O., Rossi, A., Martinez-Rossi, N.M., Almeida, F., 2018. Extracellular vesicles from the dermatophyte trichophyton interdigitalemodulate macrophage and keratinocyte functions. Front. Immunol. 9, 5–7. https://doi.org/10.3389/fimmu.2018.02343.

Borba-Santos, L.P., Visbal, G., Gagini, T., Rodrigues, A.M., De Camargo, Z.P., Lopes-Bezerra, L.M., Ishida, K., De Souza, W., Rozental, S., 2016. Δ 24 -sterol methyltransferase plays an important role in the growth and development of Sporothrix schenckii and Sporothrix brasiliensis. Front. Microbiol. 7, 1–13. https://doi.org/10.3389/fmicb.2016.00311.

Branco, M.R., Marinho, H.S., Cyrne, L., Antunes, F., 2004. Decrease of H2O2 plasma membrane permeability during adaptation to H2O2 in Saccharomyces cerevisiae. J. Biol. Chem. 279, 6501–6506. https://doi.org/10.1074/jbc.M311818200.

Brown, L., Wolf, J.M., Prados-Rosales, R., Casadevall, A., 2015. Through the wall: extracellular vesicles in Gram-positive bacteria, mycobacteria and fungi. Nat. Rev. Microbiol. 13, 620–630. https://doi.org/10.1038/nrmicro3480.

Casadevall, A., Mukherjee, J., Scharff, M.D., 1992. Monoclonal antibody based ELISAs for cryptococcal polysaccharide. J. Immunol. Methods 154, 27–35. https://doi.org/10.1016/0022-1759(92)90209-C.

Chang, Y.C., Ingavale, S.S., Bien, C., Espenshade, P., Kwon-Chung, K.J., 2009. Conservation of the sterol regulatory element-binding protein pathway and its pathobiological importance in cryptococcus neoformans. Eukaryot. Cell 8, 1770–1779. https://doi.org/10.1128/EC.00207-09.

Chen, Y.L., Lehman, V.N., Averette, A.F., Perfect, J.R., Heitman, J., 2013. Posaconazole exhibits in vitro and in vivo synergistic antifungal activity with caspofungin or FK506 against Candida albicans. PLoS ONE 8. https://doi.org/10.1371/journal.pone.0057672.

CLSI, n.d. Reference method for broth dilution antifungal susceptibility testing of yeasts; Approved standard—Third Edition. CLSI document M27-A3. Wayne, PA: Clinical and Laboratory Standards Institute; 2008.

Cowen, L.E., Lindquist, S., 2005. Cell biology: Hsp90 potentiates the rapid evolution of new traits: drug resistance in diverse fungi. Science (80-.) 309, 2185–2189. https://doi.org/10.1126/science.1118370.

Cowen, L.E., Steinbach, W.J., 2008. Stress, drugs, and evolution: The role of cellular signaling in fungal drug resistance. Eukaryot. Cell 7, 747–764. https://doi.org/10.1128/EC.00041-08.

Cox, G.M., Harrison, T.S., Mcdade, H.C., Taborda, C.P., Heinrich, G., Casadevall, A., Perfect, J.R., 2003. Superoxide dismutase influences the virulence of Cryptococcus neoformans by affecting growth within macrophages. Infect. Immun. 71, 173–180. https://doi.org/10.1128/IAI.71.1.173.

Cruz, M.C., Goldstein, A.L., 2002. Calcineurin is essential for survival during membrane stress in Candida albicans. EMBO J. 21, 546–559. https://doi.org/10.1093/emboj/21.4.546.

Daum, G., Lees, N.D., Bard, M., Dickson, R., 1998. Biochemistry, cell biology and molecular biology of lipids of Saccharomyces cerevisiae. Yeast 14, 1471–1510. https://doi.org/10.1002/(SICI)1097-0061(199812)14:16<1471::AID-YEA353>3.0.CO;2-Y.

de Toledo Martins, S., Szwarc, P., Goldenberg, S., Alves, L.R., 2018. Extracellular vesicles in fungi: composition and functions. Curr. Top. Microbiol. Immunol. 45–59. https://doi.org/10.1007/82_2018_141.

Djordjevic, J.T., 2010. Role of phospholipases in fungal fitness, pathogenicity, and drug development – lessons from Cryptococcus neoformans. Front. Microbiol. 1, 1–13. https://doi.org/10.3389/fmicb.2010.00125.

Dufourc, E.J., 2008. Sterols and membrane dynamics. J. Chem. Biol. 1, 63–77. https://doi.org/10.1007/s12154-008-0010-6.

Dupont, S., Beney, L., Ferreira, T., Gervais, P., 2011. Nature of sterols affects plasma membrane behavior and yeast survival during dehydration. Biochim. Biophys. Acta – Biomembr. 1808, 1520–1528. https://doi.org/10.1016/j.bbamem.2010.11.012.

Ermakova, E., Zuev, Y., 2017. Effect of ergosterol on the fungal membrane properties. All-atom and coarse-grained molecular dynamics study. Chem. Phys. Lipids 209, 45–53. https://doi.org/10.1016/j.chemphyslip.2017.11.006.

Espenshade, P.J., Hughes, A.L., 2007. Regulation of sterol synthesis in Eukaryotes. Annu. Rev. Genet. 41, 401–427. https://doi.org/10.1146/annurev.genet.41.110306.130315.

Farnoud, A.M., Toledo, A.M., Konopka, J.B., Del Poeta, M., London, E., 2015. Raft-like Membrane Domains in Pathogenic Microorganisms, Current Topics in Membranes. Elsevier Ltd. https://doi.org/10.1016/bs.ctm.2015.03.005.

Flowers, S.A., Barker, K.S., Berkow, E.L., Toner, G., Chadwick, S.G., Gygax, S.E., Morschhäuser, J., David Rogers, P., 2012. Gain-of-function mutations in UPC2 are a frequent cause of ERG11 upregulation in azole-resistant clinical isolates of Candida albicans. Eukaryot. Cell 11, 1289–1299. https://doi.org/10.1128/EC.00215-12.

Folch, J., Lees, M., Sloane Stanley, G., 1957. A simple method for the isolation and purification of total lipides from animal tissues. J. Biol. Chem. 226, 497–509.

Folmer, V., Pedroso, N., Matias, A.C., Lopes, S.C.D.N., Antunes, F., Cyrne, L., Marinho, H.S., 2008. H2O2 induces rapid biophysical and permeability changes in the plasma membrane of Saccharomyces cerevisiae. Biochim. Biophys. Acta – Biomembr. 1778, 1141–1147. https://doi.org/10.1016/j.bbamem.2007.12.008.

Fonseca, F.L., Frases, S., Casadevall, A., Fischman-Gompertz, O., Nimrichter, L., Rodrigues, M.L., 2009a. Structural and functional properties of the Trichosporon asahii glucuronoxylomannan. Fungal Genet. Biol. 46, 496–505. https://doi.org/10.1016/j.fgb.2009.03.003.

Fonseca, F.L., Nimrichter, L., Cordero, R.J.B., Frases, S., Rodrigues, J., Goldman, D.L., Andruszkiewicz, R., Milewski, S., Travassos, L.R., Casadevall, A., Rodrigues, M.L., 2009b. Role for chitin and chitooligomers in the capsular architecture of cryptococcus neoformansV. Eukaryot. Cell 8, 1543–1553. https://doi.org/10.1128/EC.00142-09.

Frases, S., Pontes, B., Nimrichter, L., Viana, N.B., Rodrigues, M.L., Casadevall, A., 2009. Capsule of Cryptococcus neoformans grows by enlargement of polysaccharide molecules. Proc. Natl. Acad. Sci. U.S.A. 106, 1228–1233. https://doi.org/10.1073/pnas.0808995106.

Gaber, R.F., Copple, D.M., Kennedy, B.K., Vidal, M., Bard, M., 1989. The yeast gene ERG6 is required for normal membrane function but is not essential for biosynthesis of the cell-cycle-sparking sterol. Mol. Cell. Biol. 9, 3447–3456. https://doi.org/10.1128/mcb.9.8.3447.

Gachotte, D., Barbuch, R., Gaylor, J., Nickel, E., Bard, M., 1998. Characterization of the Saccharomyces cerevisiae ERG26 gene encoding the C-3 sterol dehydrogenase (C-4 decarboxylase) involved in sterol biosynthesis. Proc. Natl. Acad. Sci. U.S.A. 95, 13794–13799. https://doi.org/10.1073/pnas.95.23.13794.

Gehrmann, U., Qazi, K.R., Johansson, C., Hultenby, K., Karlsson, M., Lundeberg, L., Gabrielsson, S., Scheynius, A., 2011. Nanovesicles from malassezia sympodialis and host exosomes induce cytokine responses – novel mechanisms for host-microbe interactions in atopic eczema. PLoS One 6, 1–10. https://doi.org/10.1371/journal.pone.0021480.

Hannich, J.T., Umebayashi, K., Riezman, H., 2011. Distribution and functions of sterols. Cold Spring Harb. Lab. Press 3, 47–62. https://doi.org/10.1101/cshperspect.a004762.

Hitchcock, C.A., Barrett-Bee, K.J., Russell, N.J., 1987. The lipid composition and permeability to azole of an azole- and polyene-resistant mutant of candida albicans. Med. Mycol. 25, 29–37. https://doi.org/10.1080/02681218780000041.

Hu, Z., He, B., Ma, L., Sun, Y., Niu, Y., Zeng, B., 2017. Recent advances in ergosterol biosynthesis and regulation mechanisms in Saccharomyces cerevisiae. Indian J. Microbiol. 57, 270–277. https://doi.org/10.1007/s12088-017-0657-1.

Huang, S.H., Wu, C.H., Chang, Y.C., Kwon-Chung, K.J., Brown, R.J., Jong, A., 2012. Cryptococcus neoformans-derived microvesicles enhance the pathogenesis of fungal brain infection. PLoS One 7. https://doi.org/10.1371/journal.pone.0048570.

Ikeda, M.A.K., De Almeida, J.R.F., Jannuzzi, G.P., Cronemberger-Andrade, A., Torrecilhas, A.C.T., Moretti, N.S., Da Cunha, J.P.C., De Almeida, S.R., Ferreira, K.S., 2018. Extracellular vesicles from sporothrix brasiliensisare an important virulence factor that induce an increase in fungal burden in experimental sporotrichosis. Front. Microbiol. 9, 1–11. https://doi.org/10.3389/fmicb.2018.02286.

Iwaki, T., Iefuji, H., Hiraga, Y., Hosomi, A., Morita, T., Giga-Hama, Y., Takegawa, K., 2008. Multiple functions of ergosterol in the fission yeast Schizosaccharomyces pombe. Microbiology 154, 830–841. https://doi.org/10.1099/mic.0.2007/011155-0.

Jacquier, N., Schneiter, R., 2012. Mechanisms of sterol uptake and transport in yeast. J. Steroid Biochem. Mol. Biol. 129, 70–78. https://doi.org/10.1016/j.jsbmb.2010.11.014.

Jensen-Pergakes, K.L., Kennedy, M.A., Lees, N.D., Barbuch, R., Koegel, C., Bard, M., 1998. Sequencing, disruption, and characterization of the Candida albicans sterol methyltransferase (ERG6) gene: Drug susceptibility studies in erg6 mutants. Antimicrob. Agents Chemother. 42, 1160–1167.

Jia, N., Arthington-Skaggs, B., Lee, W., Pierson, C.A., Lees, N.D., Eckstein, J., Barbuch, R., Bard, M., 2002. Candida albicans sterol C-14 reductase, encoded by the ERG24 gene, as a potential antifungal target site. Antimicrob. Agents Chemother. 46, 947–957. https://doi.org/10.1128/AAC.46.4.947-957.2002.

Joseph-Horne, T., Loeffler, R.S.T., Hollomon, D.W., Kelly, S.L., 1996. Amphotericin B resistant isolates of Cryptococcus neoformans without alteration in sterol biosynthesis. J. Med. Vet. Mycol. 34, 223–225. https://doi.org/10.1080/02681219680000381.

Karst, F., Lacroute, F., 1974. Yeast mutant requiring only a sterol as growth supplement. Biochem. Biophys. Res. Commun. 59, 370–376. https://doi.org/10.1016/S0006-291X(74)80216-0.

Karst, F., Lacroute, F., 1973. Isolation of pleiotropic yeast mutants requiring ergosterol for growth. Biochem. Biophys. Res. Commun. 52, 741–747. https://doi.org/10.1016/0006-291X(73)90999-6.

Kelly, S.L., Lamb, D.C., Taylor, M., Corran, A.J., Baldwin, B.C., Powderly, W.G., 1994. Resistance to amphotericin B associated with defective sterol Δ8→7 isomerase in a Cryptococcus neoformans strain from an AIDS patient. FEMS Microbiol. Lett. 122, 39–42. https://doi.org/10.1111/j.1574-6968.1994.tb07140.x.

Kim, M.S., Kim, S.Y., Yoon, J.K., Lee, Y.W., Bahn, Y.S., 2009. An efficient gene-disruption method in Cryptococcus neoformans by double-joint PCR with NAT-split markers. Biochem. Biophys. Res. Commun. 390, 983–988. https://doi.org/10.1016/j.bbrc.2009.10.089.

Kim, S.J., Kwon Chung, K.J., Milne, G.W.A., Hill, W.B., Patterson, G., 1975. Relationship between polyene resistance and sterol compositions in Cryptococcus neoformans. Antimicrob. Agents Chemother. 7, 99–106. https://doi.org/10.1128/AAC.7.1.99.

Ko, Y.J., Yu, Y.M., Kim, G.B., Lee, G.W., Maeng, P.J., Kim, S., Floyd, A., Heitman, J., Bahn, Y.S., 2009. Remodeling of global transcription patterns of Cryptococcus neoformans genes mediated by the stress-activated HOG signaling pathways. Eukaryot. Cell 8, 1197–1217. https://doi.org/10.1128/EC.00120-09.

Kodedová, M., Sychrová, H., 2015. Changes in the sterol composition of the plasma membrane affect membrane potential, salt tolerance and the activity of multidrug resistance pumps in Saccharomyces cerevisiae. PLoS One 10, 1–19. https://doi.org/10.1371/journal.pone.0139306.

Konecna, A., Toth Hervay, N., Valachovic, M., Gbelska, Y., 2016. ERG6 gene deletion modifies Kluyveromyces lactis susceptibility to various growth inhibitors. Yeast 33, 621–632. https://doi.org/10.1002/yea.

Koselny, K., Mutlu, N., Minard, A.Y., Kumar, A., Krysan, D.J., Wellington, M., 2018. A genome-wide screen of deletion mutants in the filamentous Saccharomyces cerevisiae background identifies ergosterol as a direct trigger of macrophage pyroptosis. MBio 9, e01204–e1218. https://doi.org/10.1128/mBio.01204-18.

Kristan, K., Rižner, T.L., 2012. Steroid-transforming enzymes in fungi. J. Steroid Biochem. Mol. Biol. 129, 79–91. https://doi.org/10.1016/j.jsbmb.2011.08.012.

Lafayette, S.L., Collins, C., Zaas, A.K., Schell, W.A., Betancourt-Quiroz, M., Leslie Gunatilaka, A.A., Perfect, J.R., Cowen, L.E., 2010. PKC signaling regulates drug resistance of the fungal pathogen candida albicans via circuitry comprised of mkc1, calcineurin, and hsp90. PLoS Pathog. 6, 79–80. https://doi.org/10.1371/journal.ppat.1001069.

Luna-Tapia, A., Peters, B.M., Eberle, K.E., Kerns, M.E., Foster, T.P., Marrero, L., Noverr, M.C., Fidel, P.L., Palmera, G.E., 2015. ERG2 and ERG24 are required for normal vacuolar physiology as well as Candida albicans pathogenicity in a murine model of disseminated but not vaginal candidiasis. Eukaryot. Cell 14, 1006–1016. https://doi.org/10.1128/EC.00116-15.

Lv, Q.Z., Yan, L., Jiang, Y.Y., 2016. The synthesis, regulation, and functions of sterols in Candida albicans: well-known but still lots to learn. Virulence 7, 649–659. https://doi.org/10.1080/21505594.2016.1188236.

Maziarz, E.K., Perfect, J.R., 2016. Cryptococcosis. Infect. Dis. Clin. N Am. 30, 179–206. https://doi.org/10.1007/978-3-540-75387-2_123.

McFadden, D.C., Casadevall, A., 2004. Unexpected diversity in the fine specificity of monoclonal antibodies that use the same V region gene to glucuronoxylomannan of Cryptococcus neoformans. J. Immunol. 172, 3670–3677. https://doi.org/10.4049/jimmunol.172.6.3670.

Mesa-Arango, A.C., Trevijano-Contador, N., Román, E., Sánchez-Fresneda, R., Casas, C., Herrero, E., Argüelles, J.C., Pla, J., Cuenca-Estrella, M., Zaragoza, O., 2014. The production of reactive oxygen species is a universal action mechanism of amphotericin B against pathogenic yeasts and contributes to the fungicidal effect of this drug. Antimicrob. Agents Chemother. 58, 6627–6638. https://doi.org/10.1128/AAC.03570-14.

Nes, W.D., Jayasimha, P., Song, Z., 2008. Yeast sterol C24-methyltransferase: Role of highly conserved tyrosine-81 in catalytic competence studied by site-directed mutagenesis and thermodynamic analysis. Arch. Biochem. Biophys. 477, 313–323. https://doi.org/10.1016/j.abb.2008.05.016.

Nes, W.D., Zhou, W., Ganapathy, K., Liu, J.L., Vatsyayan, R., Chamala, S., Hernandez, K., Miranda, M., 2009. Sterol 24-C-methyltransferase: An enzymatic target for the disruption of ergosterol biosynthesis and homeostasis in Cryptococcus neoformans. Arch. Biochem. Biophys. 481, 210–218. https://doi.org/10.1016/j.abb.2008.11.003.

Nichols, C.B., Fraser, J.A., Heitman, J., 2004. PAK kinases Ste20 and Pak1 govern cell polarity at different stages of mating in Cryptococcus neoformans. Mol. Biol. Cell 15, 4476–4489. https://doi.org/10.1091/mbc.E04.

Nimrichter, L., Frases, S., Cinelli, L.P., Viana, N.B., Nakouzi, A., Travassos, L.R., Casadevall, A., Rodrigues, M.L., 2007. Self-aggregation of Cryptococcus neoformans capsular glucuronoxylomannan is dependent on divalent cations. Eukaryot. Cell 6, 1400–1410. https://doi.org/10.1128/EC.00122-07.

O'Meara, T.R., Norton, D., Price, M.S., Hay, C., Clements, M.F., Nichols, C.B., Alspaugh, J.A., 2010. Interaction of Cryptococcus neoformans Rim101 and protein kinase a regulates capsule. PLoS Pathog. 6. https://doi.org/10.1371/journal.ppat.1000776.

Oliveira, D.L., Nakayasu, E.S., Joffe, L.S., Guimarães, A.J., Sobreira, T.J.P., Nosanchuk, J.D., Cordero, R.J.B., Frases, S., Casadevall, A., Almeida, I.C., Nimrichter, L., Rodrigues, M.L., 2010. Characterization of yeast extracellular vesicles: evidence for the participation of different pathways of cellular traffic in vesicle biogenesis. PLoS ONE 5, 1–13. https://doi.org/10.1371/journal.pone.0011113.

Onyewu, C., Blankenship, J.R., Del Poeta, M., Heitman, J., 2003. Ergosterol biosynthesis inhibitors become fungicidal when combined with calcineurin inhibitors against Candida albicans, Candida glabrata, and Candida krusei. Antimicrob. Agents Chemother. 47, 956–964. https://doi.org/10.1128/AAC.47.3.956-964.2003.

Parks, L.W., Casey, W.M., 1995. Physiological implications of sterol biosynthesis in yeast. Annu. Rev. Microbiol. 49, 95–116. https://doi.org/10.1146/annurev.mi.49.100195.000523.

Peleg, A.Y., Jara, S., Monga, D., Eliopoulos, G.M., Moellering, R.C., Mylonakis, E., 2009. Galleria mellonella as a model system to study Acinetobacter baumannii pathogenesis and therapeutics. Antimicrob. Agents Chemother. 53, 2605–2609. https://doi.org/10.1128/AAC.01533-08.

Pfaller, M.A., Messer, S.A., Boyken, L., Rice, C., Tendolkar, S., Hollis, R.J., Doern, G.V., Diekema, D.J., 2005. Global trends in the antifungal susceptibility of Cryptococcus neoformans (1990 to 2004). J. Clin. Microbiol. 43, 2163–2167. https://doi.org/10.1128/JCM.43.5.2163-2167.2005.

Price, M.F., Wilkinson, I.D., Gentry, L.O., 1982. Plate method for detection of phospholipase activity in Candida albicans. Med. Mycol. 20, 7–14. https://doi.org/10.1080/00362178285380031.

Proszynski, T.J., Klemm, R.W., Gravert, M., Hsu, P.P., Gloor, Y., Wagner, J., Kozak, K., Grabner, H., Walzer, K., Bagnat, M., Simons, K., Walch-Solimena, C., 2005. A genome-wide visual screen reveals a role for sphingolipids and ergosterol in cell surface delivery in yeast. Proc. Natl. Acad. Sci. U.S.A. 102, 17981–17986. https://doi.org/10.1073/pnas.0509107102.

Rajasingham, R., Smith, R.M., Park, B.J., Jarvis, J.N., Govender, N.P., Chiller, T.M., Denning, D.W., Loyse, A., Boulware, D.R., 2017. Global burden of disease of HIV-associated cryptococcal meningitis: an updated analysis. Lancet Infect. Dis. 17, 873–881. https://doi.org/10.1016/S1473-3099(17)30243-8.

Reis, F.C.G., Borges, B.S., Jozefowicz, L.J., Sena, B.A.G., Garcia, A.W.A., Medeiros, L.C., Martins, S.T., Honorato, L., Schrank, A., Vainstein, M.H., Kmetzsch, L., Nimrichter, L., Alves, L.R., Staats, C.C., Rodrigues, M.L., 2019. A novel protocol for the isolation of fungal extracellular vesicles reveals the participation of a putative scramblase in polysaccharide export and capsule construction in cryptococcus gattii. mSphere 4, 1–15. https://doi.org/10.1128/msphere.00080-19.

Robbins, N., Caplan, T., Cowen, L.E., 2017. Molecular evolution of antifungal drug resistance. Annu. Rev. Microbiol. 71, 753–775. https://doi.org/10.1146/annurev-micro-030117-020345.

Rodrigues, M.L., 2018. The multifunctional fungal ergosterol. MBio 9, e01755–e1818. https://doi.org/10.1128/mBio.01755-18.

Rodrigues, M.L., Nakayasu, E.S., Oliveira, D.L., Nimrichter, L., Nosanchuk, J.D., Almeida, I.C., Casadevall, A., 2008. Extracellular vesicles produced by Cryptococcus neoformans contain protein components associated with virulence. Eukaryot. Cell 7, 58–67. https://doi.org/10.1128/EC.00370-07.

Rodrigues, M.L., Nimrichter, L., Oliveira, D.L., Frases, S., Miranda, K., Zaragoza, O., Alvarez, M., Nakouzi, A., Feldmesser, M., Casadevall, A., 2007. Vesicular polysaccharide export in Cryptococcus neoformans is a eukaryotic solution to the problem of fungal trans-cell wall transport. Eukaryot. Cell 6, 48–59. https://doi.org/10.1128/EC.00318-06.

Sanglard, D., Ischer, F., Parkinson, T., Falconer, D., Bille, J., 2003. Candida albicans mutations in the ergosterol biosynthetic pathway and resistance to several antifungal agents. Antimicrob. Agents Chemother. 47, 2404–2412. https://doi.org/10.1128/AAC.47.8.2404.

Servouse, M., Karst, F., 1986. Regulation of early enzymes of ergosterol biosynthesis in Saccharomyces cerevisiae. Biochem. J. 240, 541–547. https://doi.org/10.1042/bj2400541.

Siafakas, A.R., Sorrell, T.C., Wright, L.C., Wilson, C., Larsen, M., Boadle, R., Williamson, P.R., Djordjevic, J.T., 2007. Cell wall-linked cryptococcal phospholipase B1 is a source of secreted enzyme and a determinant of cell wall integrity. J. Biol. Chem. 282, 37508–37514. https://doi.org/10.1074/jbc.M707913200.

Silver, P.M., Oliver, B.G., White, T.C., 2004. Role of Candida albicans transcription factor Upc2p in drug resistance and sterol metabolism. Eukaryot. Cell 3, 1391–1397. https://doi.org/10.1128/EC.3.6.1391-1397.2004.

Toffaletti, D.L., Rude, T.H., Johnston, S.A., Durack, D.T., Perfect, J.R., 1993. Gene transfer in Cryptococcus neoformans by use of biolistic delivery of DNA. J. Bacteriol. 175, 1405–1411. https://doi.org/10.1128/jb.175.5.1405-1411.1993.

Toh-e, A., Ohkusu, M., Shimizu, K., Yamaguchi, M., Ishiwada, N., Watanabe, A., Kamei, K., 2017. Creation, characterization and utilization of Cryptococcus neoformans mutants sensitive to micafungin. Curr. Genet. 63, 1093–1104. https://doi.org/10.1007/s00294-017-0713-8.

Umebayashi, K., Nakano, A., 2003. Ergosterol is required for targeting of tryptophan permease to the yeast plasma membrane. J. Cell Biol. 161, 1117–1131. https://doi.org/10.1083/jcb.200303088.

Vallejo, M.C., Nakayasu, E.S., Longo, L.V.G., Ganiko, L., Lopes, F.G., Matsuo, A.L., Almeida, I.C., Puccia, R., 2012. Lipidomic analysis of extracellular vesicles from the pathogenic phase of Paracoccidioides brasiliensis. PLoS One 7, 1–10. https://doi.org/10.1371/journal.pone.0039463.

Vandeputte, P., Tronchin, G., Bergès, T., Hennequin, C., Chabasse, D., Bouchara, J.P., 2007. Reduced susceptibility to polyenes associated with a missense mutation in the ERG6 gene in a clinical isolate of Candida glabrata with pseudohyphal growth. Antimicrob. Agents Chemother. 51, 982–990. https://doi.org/10.1128/AAC.01510-06.

Vargas, G., Rocha, J.D.B., Oliveira, D.L., Albuquerque, P.C., Frases, S., Santos, S.S., Nosanchuk, J.D., Gomes, A.M.O., Medeiros, L.C.A.S., Miranda, K., Sobreira, T.J.P., Nakayasu, E.S., Arigi, E.A., Casadevall, A., Guimaraes, A.J., Rodrigues, M.L., Freire-de-Lima, C.G., Almeida, I.C., Nimrichter, L., 2015. Compositional and immunobiological analyses of extracellular vesicles released by Candida albicans. Cell. Microbiol. 17, 389–407. https://doi.org/10.1111/cmi.12374.

Vincent, B.M., Lancaster, A.K., Scherz-Shouval, R., Whitesell, L., Lindquist, S., 2013. Fitness trade-offs restrict the evolution of resistance to Amphotericin B. PLoS Biol. 11. https://doi.org/10.1371/journal.pbio.1001692.

Visbal, G., San-Blas, G., Maldonado, A., Álvarez-Aular, Á., Capparelli, M.V., Murgich, J., 2011. Synthesis, in vitro antifungal activity and mechanism of action of four sterol hydrazone analogues against the dimorphic fungus Paracoccidioides brasiliensis. Steroids 76, 1069–1081. https://doi.org/10.1016/j.steroids.2011.04.012.

Wachtler, V., Balasubramanian, M.K., 2006. Yeast lipid rafts? An emerging view. Trends Cell Biol. 16, 1–4. https://doi.org/10.1016/j.tcb.2005.11.008.

Walton, F.J., Idnurm, A., Heitman, J., 2005. Novel gene functions required for melanization of the human pathogen Cryptococcus neoformans. Mol. Microbiol. 57, 1381–1396. https://doi.org/10.1111/j.1365-2958.2005.04779.x.

Weete, J.D., Abril, M., Blackwell, M., 2010. Phylogenetic distribution of fungal sterols. PLoS One 5, 3–8. https://doi.org/10.1371/journal.pone.0010899.

White, T.C., 1997. Increased mRNA levels of ERG16, CDR, and MDR1 correlate, with increases in azole resistance in Candida albicans isolates from a patient infected with human immunodeficiency virus. Antimicrob. Agents Chemother. 41, 1482–1487. https://doi.org/10.1128/aac.41.7.1482.

Xie, J.L., Polvi, E.J., Shekhar-Guturja, T., Cowen, L.E., 2014. Elucidating drug resistance in human fungal pathogens. Future Microbiol. 9, 523–542. https://doi.org/10.2217/fmb.14.18.

Young, L.Y., Hull, C.M., Heitman, J., 2003. Disruption of ergosterol biosynthesis confers resistance to amphotericin B in Candida lusitaniae. Antimicrob. Agents Chemother. 47, 2717–2724. https://doi.org/10.1128/AAC.47.9.2717-2724.2003.

Zamith-Miranda, D., Nimrichter, L., Rodrigues, M.L., Nosanchuk, J.D., 2018. Fungal extracellular vesicles: modulating host–pathogen interactions by both the fungus and the host. Microbes Infect. 20, 501–504. https://doi.org/10.1016/j.micinf.2018.01.011.

Zaragoza, O., Rodrigues, M.L., De Jesus, M., Frases, S., Dadachova, E., Casadevall, A., 2009. The capsule of the fungal pathogen cryptococcus neoformans. Adv. Appl. Microbiol. https://doi.org/10.1016/S0065-2164(09)01204-0.

Zhang, Y.Q., Rao, R., 2010. Beyond ergosterol: linking ph to antifungal mechanisms. Virulence 1, 551–554. https://doi.org/10.4161/viru.1.6.13802.